LAMINAR AIR FLOW SUPER WINDOW

RENEWABLE ENERGY BRANCH

PREPARED FOR:

Renewable Energy Branch
Energy, Mines and Resources Canada
Ottawa, Canada
DSS Contract File No.: 57SZ.23216-6-6093
FILE: 6179,DD#41
June 10, 1987

PREPARED BY:

G. K. Yuill and Associates Ltd.
1441 Pembina Highway
Winnipeg, Manitoba
R3T 2C4
Telephone: (204) 474-2461

SCIENTIFIC AUTHORITY:

Passive Solar Technology Coordinator
Renewable Energy Branch
Department Energy, Mines and Resources
4th Floor, 460 O'Connor Street
Ottawa, Ontario
K1A 0E4

TABLE OF CONTENTS

	ACKNOWLEDGMENTS	i
	PREFACE	ii
	ABSTRACT	iv
	EXECUTIVE SUMMARY	v
1.0	INTRODUCTION	1
1.1	The Laminar Air Flow Super Window Concept	1
1.2	Literature Search	1
2.0	OBJECTIVES	4
3.0	ANALYSIS OF THE THERMAL PERFORMANCE OF THE LAMINAR AIR FLOW SUPER WINDOW	6
3.1	Introduction	6
3.2	Heat Transfer Equations and Thermal Models	7
3.3	Simplified Computer Modeling to Predict the Thermal Performance of the LAFSW	13
3.3.1	Description of the Slug Flow Model	13
3.3.2	Comparison of the Ratio of Fluxes at y=0 and y=L Plates	18
3.3.3	Comparison of Local Nusselt Numbers	19
3.3.4	Window Dimensions	25
3.3.5	Window Performance Simulation	27
3.3.5.1	Approach	27
3.3.5.2	Window Performance without Solar Radiation	27
3.3.5.3	Window Performance with Solar Radiation	27
3.4	Detailed Computer Modeling to Predict the Thermal Performance of the LAFSW	30
3.4.1	The Computer Model	30
3.4.2	Predicted Thermal Performance of LAFSW Using Detailed Computer Simulation Program	41
3.4.2.1	Validation of the Assumptions in the LAFSW Model	41
3.4.2.2	Comparison with Approximate Analysis	43
3.4.2.3	LAFSW Configuration Simulated	43

4.0	DEVELOPMENT AND INSTALLATION OF PROTOTYPE WINDOW	55
4.1	The Prototype Window Design	55
4.2	Installation of the Prototype	55
5.0	VENTILATION SYSTEM	58
5.1	Initial Review	58
5.2	Humidity Controlled Air Inlets	59
5.3	Cost Analysis	61
6.0	DISCUSSIONS WITH MANUFACTURERS	63
7.0	INTERPRETATION OF THE PROJECT RESULTS	64
7.1	Theoretical and Practical Feasibility of the Window Concept	64
7.2	Economic Feasibility	65
7.3	Continuation to Second Phase of LAFSW Evaluation	65
8.0	CONCLUSIONS	67
9.0	RECOMMENDATIONS	68
	REFERENCES	69
	APPENDIX A	

LIST OF TABLES

Table 3.1	Flux Ratios, Constant Temperature and Constant Flux	20
Table 3.2	Super Window Performance, with low E coatings	32
Table 3.3	Super Window Performance for Different Dimensions and Gap Widths and a Supply Air Flow Rate of 35 l/s	45
Table 3.4	Window Width Required to Provide a Ventilation Rate of 35 l/s for a Nominal Grashof-to-Reynolds Number Ratio of 12	47
Table 3.5	Super Window Performance for Different Dimensions and Gap Widths, a Supply Air Flow Rate of 35 l/s and a Low Emittance Coating on the Outside Surface of the Middle Pane	51
Table 3.6	Energy Saving Rates and Cost Savings Achieved by Different Laminar Air Flow Gaps	54

LIST OF FIGURES

Figure 3.1	Laminar Air Flow Super Window Layout (adapted from Reference 9)	9
Figure 3.2	Diagram of boundary conditions for slug flow model	15
Figure 3.3	Local Nusselt numbers at the y=0 and y=1 plate, for the slug flow case with either constant temperature or constant heat flux boundary conditions	21
Figure 3.3a	Temperature distribution, constant temperature with slug flow at large x*	22
Figure 3.4	Local Nusselt numbers at the y=0 and y=L plate, for both the slug flow and the fully developed air flow conditions	24
Figure 3.5	Finite difference grid network in the laminar air flow gap	33
Figure 3.6	Relationships between the physical coordinate, x, the stretched coordinate, x, the stretching factor, ϵ, for flow between parallel plates (from reference 24)	33
Figure 3.7	Investigation of the Effect of Heat Conduction along the Glazings	42
Figure 3.8	Temperature Profiles Across the Laminar Air Flow Gap for 1-m by 10-m Window with 9-mm Gap and Nighttime Simulation Conditions	48
Figure 3.9	Temperature Profiles Across the Laminar Air Flow Gap for 1-m by 10-m Window with 9-mm Gap and Daytime Simulation Conditions	49
Figure 4.1	Vertical cross-sectional view of prototype laminar air flow window. The window ducting is not shown in this view.	56
Figure 4.2	The LAFSW in Place	57
Figure 4.2a	Interior View Showing Ducting, Fan and Heater	57
Figure 4.2b	Exterior View LAFSW on Right	57

ACKNOWLEDGMENTS

The work described in this report was supported by the Renewable Energy Branch of Energy Mines and Resources Canada. The co-operative supervision of Mr. Tim Mayo, the project's Scientific Authority, was very helpful.

Mr. Dan Friesen of Willmar Windows provided valuable guidance in the development of a simple and economical design for the laminar air flow super window.

Disclaimer

This report is distributed for informational purposes only and does not necessarily reflect the views of the Government of Canada nor constitute an endorsement of any commercial product or person. Neither Canada nor its ministers, officers, employees or agents makes any warranty in respect of this report or assumes any liability arising out of this report.

PREFACE

This report describes the first phase of a project to develop a commercially viable laminar air flow super window (LAFSW). The purpose of this part of the project was to determine whether or not the LAFSW was theoretically and economically feasible and whether or not there were any practical barriers to its use.

There were three main elements to this project. The first was the use of an approximate analysis of the heat transfer problem to determine the appropriate size range for the window. The second was the development of a computer program to do more precise analysis of the heat transfer problem. The third was the construction and installation of an LAFSW to check for any practical difficulties that might arise.

An LAFSW consists of three panes of glass. The inner two panes are sealed. There is a slot at the bottom of the window for outside air to enter the space between the outer and middle panes. There is another slot at the top of the window to duct this air from between the two panes into the house. The heat which is lost through the two inner panes is thus recaptured by the stream of air flowing between the outer and middle panes. If ventilation air is introduced into the house through an LAFSW it will be thus preheated.

In concept, it would appear to be possible to eliminate completely any convective heat transfer between the outer panes of an LAFSW, by drawing off the laminar air stream at the top just before the thermal boundary layer reached the outer pane. In this project, the detailed heat transfer analysis has shown how close it is possible to come to that ideal LAFSW.

Others have analyzed LAFSWs in the past. The two major advances of this project have been that the heat transfer analysis has been much more precise and that an LAFSW has been built and installed in a house to determine its practicability. This project has developed the LAFSW concept to the point where it should now be possible to convince a

manufacturer of the economic potential of the LAFSW and to proceed with commercial development.

ABSTRACT

The objectives of this project were to develop methods of precisely analyzing the thermal performance of a laminar air flow super window (LAFSW), to use these methods to develop a practical window design and to build and install a window of this design.

Two methods of analysis were developed. The first, a simplified method, assumed that slug flow occurred in the air stream between the panes and that the heat flux along each of the panes was constant. The second more detailed method of analysis used a finite difference computer program to analyze the heat transfer in the hydrodynamically and thermally developing flow.

The analysis showed that an LAFSW could be built to match normal window dimensions and normal house ventilation requirements. The predicted energy savings justified the extra cost of the LAFSW.

The LAFSW which was built and installed worked successfully, with no practical problems developing.

EXECUTIVE SUMMARY

1.0 OBJECTIVE OF THE PROJECT

This project was the first step in the commercial development of a laminar air flow super window (LAFSW). The overall objective is to develop a window which will lose far less heat than a conventional window and which can be manufactured at a cost which will make it economically feasible. The objectives of the present project were to develop a precise analytical method to analyze the thermal performance of the LAFSW, to use this method to investigate the various window design parameters and to determine the optimum window design, and to build an LAFSW and install it in a house, to check it for unexpected practical problems.

2.0 ANALYTICAL APPROACHES TAKEN

Two approaches were taken to analyzing the heat transfer in the LAFSW. In the first approach, the heat transfer in the flowing air between the panes was analyzed for three different simple cases. These were:

1. slug flow with constant temperature at both walls;
2. slug flow with constant heat flux at one wall and constant temperature on the other wall; and
3. fully-developed flow with constant temperature at both walls.

It was found that the overall heat transfer predicted was almost the same for the two cases with constant temperature walls, one with slug flow and one with fully-developed flow. There was approximately 30% difference between the heat transfer rates predicted for the cases of constant wall heat flux and constant temperature when slug flow was assumed. The reasonably close agreement between these three cases indicated that all were good approximations to the actual heat transfer process.

The solution of the overall heat transfer problem was obtained by using the VISION computer program [9] to analyze the heat transfer through the three panes of the window, and to use the slug flow-constant heat flux solution to generate the heat fluxes required by VISION at the two surfaces of the flow channel. Since this solution required as inputs the surface temperatures at these two surfaces, the overall analytical process required an iteration between the VISION program and the slug flow-constant heat flux solution.

The increases in window thermal resistance which were predicted by this analysis were very substantial. As would be expected, the highest thermal resistance was obtained for a window with a low-E coating on the outside of the middle pane. This was RSI = 2.5 m^2k/W, compared with RSI = .45 m^2K/W for a conventional triple glazed window.

Wright [10] carried out a similar analysis using VISION and a different heat transfer model. This model was based on fully developed flow between isothermal walls. Wright evidently did not optimize the window geometry and flow rate to obtain the lowest possible heat flux from the air stream to the outer pane. He predicted substantial increases in window thermal resistance, but not as great as were predicted in the present study.

In the second approach to the analysis of the heat transfer in the flowing air stream, a finite different computer program called LAMWIN was written to calculate the temperature field and the resulting heat transfer rates. The developing velocity field was calculated using a method developed by Sparrow, Lin and Lundgren [24].

The boundary conditions at each station along the flow channel were calculated by applying the heat transfer analysis of the VISION program to each segment along the channel. This approach assumed that conductive heat transfer along the panes of glass was insignificant, and that the temperature gradient along the opposite pane did not change the radiant flux on a segment of the pane. These two assumptions were

tested by detailed analysis and were found to have an insignificant effect on the results.

The LAMWIN program was verified by several manual order-of-magnitude calculations and heat balance checks, and by comparing its predictions with those of the simplified analysis procedure previously described. The agreement between the overall window thermal resistances predicted by LAMWIN and by the slug flow - constant heat flux solution was good. The differences were of the same magnitude as the differences between the constant temperature and constant heat flux solutions.

At the time that LAMWIN was being used to analyze the performance of the LAFSW, it was assumed that the objective was to achieve the highest possible outlet temperature, to defrost a heat recovery ventilator. Therefore the Reynolds Number was minimized within the feasible range. This resulted in much lower thermal resistances than had been predicted by the simplified analysis, where thermal resistance rather than temperature rise was optimized. Thus the highest thermal resistance predicted by these LAMWIN analyses was 1.2 m^2K/W, slightly more than twice as high as for a conventional triple glazed window, but less than half as high as predicted by the simplified analysis, in which higher flow rates were used. These differences were due only to the flow rate difference, not to the method of analysis used.

Based on the LAMWIN results, annual savings were calculated for 10 m^2 of LAFSW, compared with a conventional triple glazed window. These were $74.00 per year, for the case of a 10.7 mm gap width. This is the equivalent of a present value of $550.00. These results are based on Manitoba's electricity price of .03/kWh. They would be greater in other parts of Canada.

3.0 TEST WINDOW

A test LAFSW was built to the dimensions suggested by the analysis done in the previous section. This window was installed in a house in Winnipeg and operated over the winter season of 1986 - 87. Its purpose

was not to provide thermal performance data, but simply to test the LAFSW concept for practical feasibility.

When the LAFSW was first installed, it had no suction fan on it, and the house's stack effect caused airflow out through the air inlet passage. This produced some frosting between the panes, and icicles hanging from inlet opening. These problems disappeared when the fan was installed and normal operation started. A second problem, easily remedied, was caused by air leakage through a crack between two imperfectly fitted strips of wood. No other difficulties were encountered.

4.0 ECONOMICS

Willmar Windows estimated the extra cost of building the LAFSW as about $40 for a 1-m by 1-m window. The present value of the saving was estimated at $53.70 per m^2, so the LAFSW appears to be economically feasible. In most of Canada, heating costs are higher, so the net benefit will be greater.

5.0 VENTILATION SYSTEM

The greatest difficulty with the LAFSW system is that the fresh air is introduced in small amounts at many locations. It is expensive to collect it for utilization. Several different systems were considered in this project, but all were so expensive as to make the economics of the LAFSW system marginal. Finally, after the project was essentially complete, a ventilation system was found which combines very well with the LAFSW. This is the "humidity controlled air inlet" (HCAI) system.

This system uses a humidity controlled exhaust fan to maintain the relative humidity of the exhaust air at a set value. This exhaust fan is not controlled by an "on-off" humidistat. It is proportionally controlled so that it runs continuously. It therefore maintains the house at a negative pressure. This negative pressure draws air in

through an HCAI in each room. These inlets require no power to operate. They open up to supply more air to the occupied rooms where the humidity is high, and close down when the room is unoccupied.

Obviously, the HCAI system combines well with the LAFSW, since each window can have an HCAI installed on its air outlet. Since the HCAI can be economically justified on its own, no additional cost for air distribution need be assessed to the LAFSW. At the same time, the preheating effect of the LAFSW reduces the problem which the HCAI may face in colder climates of creating uncomfortable drafts in the coldest weather.

6.0 CONCLUSIONS

The LAFSW is technically feasible and economically feasible. Its best prospect for success in houses in combination with a HCAI ventilation system.

7.0 FURTHER WORK REQUIRED

The second phase of this project should include three main elements. The first is the construction of another LAFSW, for detailed laboratory testing, to determine whether or not its performance is consistent with the prediction of LAMWIN. The second is the testing, in a house, of the combined LAFSW/HCAI system. The third is the development of the capability of simulating the operation of the LAFSW/HCAI ventilation system, so that the results of the tests can be extended to apply to other house and window configurations.

1.0 INTRODUCTION

1.1 The Laminar Air Flow Super Window Concept

The laminar air flow super window (LAFSW) is one which has an air passage between its panes through which ventilation air can be brought into a room. The object is to preheat this ventilation air. There are two general types of LAFSWs. One type has a venetian blind in the air passage between the panes. The other type does not. The window with venetian blinds offers advantages in the control of light and in the control of solar heat gain, but it has no advantage in the amount of solar energy it can collect. It has the disadvantage that it is considerably more expensive.

The goal of the present project was to develop a LAFSW of the simpler type, without an inter-pane venetian blind. It was realized that, if the air flow between the two outer panes was kept laminar, convective heat transfer from the center pane to the outer pane could be almost completely eliminated. All the heat convected into the air stream would be brought back into the building in the ventilation air. Only the heat radiated from the middle pane to the outer pane would be lost through the window. Such a window could have a thermal resistance much higher than a conventional triple glazed window.

The major task of the present project was to analyze the thermal performance of such a window, and to optimize the window design to maximize this performance. A second task was to build and install a prototype window to detect practical difficulties, and a third task was to develop a mechanical system which could use the air flowing through the LAFSW to ventilate the house.

1.2 Literature Search

A literature search was performed to support the development of the LAFSW. The search took two broad phases: the determination of other approaches to the LAFSW and the location of work regarding heat

transfer with simultaneously developing thermal and velocity boundary layers between parallel plates.

Several references were located regarding other approaches to the LAFSW. These usually took the form of air flow between glazings passing over a set of blinds [1],[2],[3],[4],[4],[6],[7]. This would cause turbulent air flow, and the approach was not examined in great detail. An early analysis of a LAFSW [8] was not entirely accurate, since the assumption was made that the glazings adjacent to the air flow were isothermal, which would not be the case in practice due to varying convective heat transfer coefficients caused by a developing thermal boundary layer.

VISION [9] is a computer model for the simulation of heat transfer in windows. It has been applied to LAFSW modeling [10]. In this latter work, it was assumed that all the glazings were isothermal and that the air flow between the glazings was fully developed. VISION provided a basis for the computer program to be developed in the present project, which would extend the heat transfer analysis from one dimension to two allow the analysis of a more realistic window model. This model included the variation of temperature along the panes of glass and the development of the velocity and temperature profiles in the air flow between the panes.

Several papers describing solutions for convective heat transfer coefficients for a developing thermal boundary layer were located [11],[12],[13],[14],[15],[16]. These papers assume fully developed flow between parallel plates, which is not directly applicable, but they were useful as a review of the possible approaches to developing a model for the present analysis.

Several papers were found which dealt with the calculation of convective heat transfer in the fluid and thermal developing region between parallel plates [17],[18],[19]. While not directly usable because of assumptions of isothermal wall or uniform heat flux conditions, these approaches provided solutions which approximated that

of the present case and put bounds on the range of results to be expected. As well, a paper that performs an analysis of heat transfer in the developing region with both convective and radiative components [20] presented an approach to an analysis of the performance of the LAFSW in the presence of solar radiation.

Hatton and Turton [21] analyzed thermally developing flow between isothermal walls at different temperatures. The velocity profile was fully developed. Their results proved to be directly applicable as an approximation to the solution of the present problem.

Tjelflaat and Bergesen [22] investigated LAFSWs experimentally and analytically. They concentrated on double pane windows, with parallel hot and cold air streams injected between them. They found that this approach produced instabilities in the flow and was complicated and expensive. They also built a triple pane window and made some preliminary measurements, but these were not conclusive. They did not analyze the triple pane window. They reported that hydrodynamic instability will occur, in fully developed channel flow between walls at different temperatures, when the ratio of the Grashof Number to the Reynolds Number is over 24.

Sparrow, Lin and Lundgren [24] presented a solution of the hydrodynamic entrance region problem for parallel flat plates. Since the temperature variations are small in the present case, the thermal and hydrodynamic problems can be treated as uncoupled, so that Sparrow, Lin and Lundgren's solution provided the developing velocity distribution required as an input to the analysis of the temperature field. Several other researchers [25,26,27,28] provided solutions to the same problem which served to verify the accuracy of the results obtained by the method of Sparrow, Lin and Lundgren.

Edwards [23] presented a useful means of calculating the optical properties of multi-pane windows.

2.0 OBJECTIVES

The overall objective of the present project was to develop the concept of the LAFSW to the point where it could be presented to a window manufacturer. To attract the attention of a manufacturer it would be necessary to provide him with estimates of the cost of the proposed system and the energy savings, and to show to him that the idea was practical and could be implemented in a house without any unexpected difficulties.

To accomplish this objective, it was necessary to carry out the following tasks:

1. Develop a computer program that could analyze the heat transfer and fluid flow in the air stream in the window, and from these results could predict the window's overall thermal performance.

2. Use this computer program to optimize the window design, considering the practical limits on window dimensions.

3. Design, construct and install a prototype window, to observe any practical problems which might arise with this kind of window.

4. Develop a method of drawing air through the window and utilizing the air for ventilation in the house.

5. Analyze the economics of the proposed window and ventilation system.

6. Present this information to an appropriate manufacturer and, if possible, obtain his involvement in the second phase of the project.

The following chapters describe how this project was carried out to achieve these objectives. Chapter 3 describes the development of the

computer program and its use to optimize the window design. Chapter 4 describes the design construction and installation of the prototype window. In Chapter 5, the ventilation system to be used with the LAFSW is described. Chapter 6 is an interpretation of the results of the project including an assessment of its economic potential.

3.0 ANALYSES OF THE THERMAL PERFORMANCE OF THE LAMINAR AIR FLOW SUPER WINDOW

3.1 Introduction

Two approaches were taken to model the thermal performance of a triple-glazed LAFSW which utilizes a laminar air flow layer in the gap between the middle and exterior panes. The first approach was based on a simple approximate solution. The second was based on a more complex exact analysis.

The principal modes of heat transfer which take place in such a window are as follows:

(i) laminar forced convection in the gap between the middle and exterior panes;
(ii) forced convection due to wind on the outdoor surface of the exterior pane;
(iii) free convection in the gap between the interior and middle panes and on the indoor surface of the interior pane;
(iv) conduction in a vertical direction along the window panes;
(v) long-wave radiation exchange between the window panes and the surroundings.

Solution of the problem involving all of the above modes of heat transfer is quite complex. In the first approach, an approximate solution to the problem was obtained by assuming that negligible temperature gradients exist along the panes of the LAFSW and that the flow in the laminar air layer is constant velocity (slug flow). This approach is discussed in Section 3.3. In the second approach, a computer program was developed which obtains a more exact solution to the heat transfer problem. It accounts for the developing velocity profile in the laminar air flow gap and uses finite difference forms of the governing heat transfer equations to solve for the temperature gradients along the glazings. This second approach is discussed in Section 3.4.

3.2 Heat Transfer Equations and Thermal Models

This section summarizes the heat transfer equations and thermal models which were used to predict the performance of the LAFSW.

The energy equation for two-dimensional, incompressible, laminar flow of a viscous fluid neglecting viscous dissipation is given as

$$u\,(\partial T/\partial x) + v\,(\partial T/\partial y) = \alpha(\partial^2 T/\partial x^2 + \partial^2 T/\partial y^2) \qquad (3.1)$$

where

u is the x-direction velocity component [m/s],
v is the y-direction velocity component [m/s],
T is the fluid temperature [K],
and α is the thermal diffusivity of the fluid [m^2/s].

In a thermal boundary layer developing along a surface, the temperature gradient in the y direction normal to the surface (refer to Figure3.1) is usually much greater than the gradient in the x direction parallel to the surface, and therefore the first term on the right hand side of the equation is often neglected, giving

$$u\,(\partial T/\partial x) + v\,(\partial T/\partial y) = \alpha(\partial^2 T/\partial y^2) \qquad (3.2)$$

This equation was used to solve for the temperature distribution in the laminar air flow gap given the velocity distribution and the appropriate thermal conditions at the boundaries of the gap. Equation 3.2 was also applicable in the case where slug flow was assumed in the laminar air flow gap since the air gap is fairly thin and subjected to a fairly large temperature difference across its edges, and therefore $\partial^2 T/\partial y^2$ could be assumed to be much greater than $\partial^2 T/\partial x^2$.

In the present analyses, algorithms and computer subroutines to calculate long-wave radiation heat transfer between glazings and the surroundings and convective heat transfer to/from the glazings were adapted from the VISION computer program [9]. VISION was developed for the Solar Energy Program of the National Research Council to evaluate

and optimize the thermal performance of super windows which incorporate a variety of energy conserving features. The heat transfer equations and thermal models from the VISION program which were relevant to the present analyses are briefly summarized as follows.

The physical layout of the triple-glazed LAFSW is shown in Figure 3.1. Included in this figure is the coordinate system used for the analysis of the laminar air flow layer. Note that the coordinate system used in the simplified analysis discussed in Section 3.3 is different from that used in the detailed analysis discussed in Section 3.4. Subscripts are used to identify the window system elements: 1 refers to the indoor environment; 2 to the interior glazing; 3 to the middle glazing; 4 to the exterior glazing; and 5 to the outdoor environment. Demfinitions of the symbols used in the figure are as follows:

TAS_i is the thickness of the air gap between glazings i and (i+1) [m];

$TEMP_1$ is the ambient indoor temperature [K];

$TEMP_5$ is the ambient outdoor temperature [K];

$TEMP_i$ is the temperature of glazing i [K];

EU_i is the hemispherical long-wave emittance of the outward facing surface of glazing i [-];

ED_i is the hemispherical long-wave emittance of the inward facing surface of glazing i [-];

RU_i is the hemispherical long-wave reflectance of the outward facing surface of glazing i [-];

RD_i is the hemispherical long-wave reflectance of the outward facing surface of glazing i [-];

JU_i is the outward radiosity for element i [W/m^2];

JD_i is the inward radiosity for element i [W/m^2];

q''_i is the total long-wave radiative plus conductive/convective heat transfer rate across the air layer between elements i and (i + 1), except between glazings 3 and 4 [W/m^2];

q''_{r34} is the long-wave radiative heat transfer between glazing 3 and 4 [W/m^2];

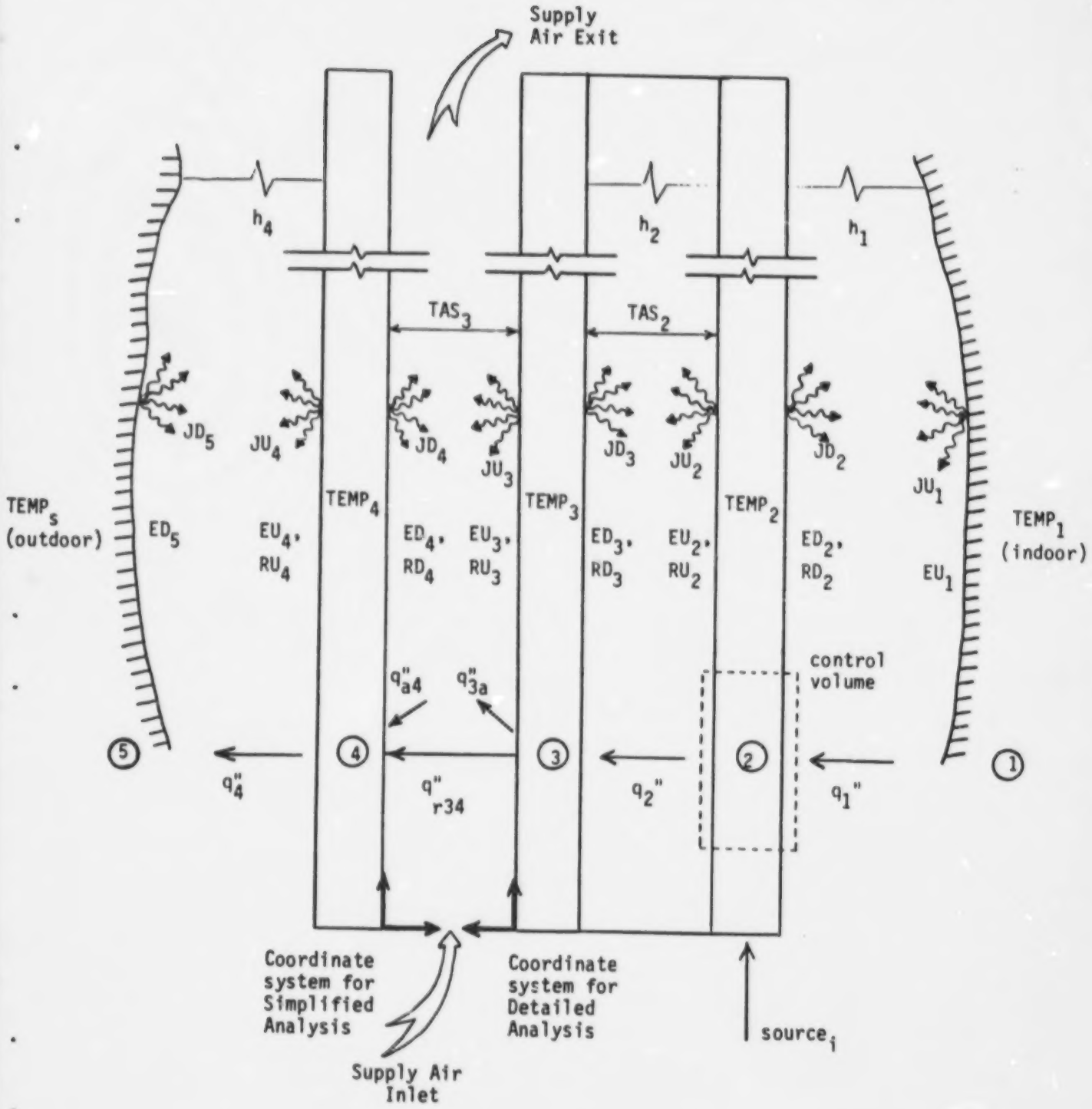

Figure 3.1 Laminar Air Flow Super Window Layout (adapted from Reference 9)

q''_{3a} is the forced convective/conductive heat transfer rate from glazing 3 to the laminar air flow layer [W/m^2];

q''_{a4} is the forced convective/conductive heat transfer rate from the laminar air flow layer to glazing 4 [W/m^2];

$SOURCS_i$ is a source term used to represent the solar radiation absorbed by glazing i [W/m^2];

and h_i is the standard conductive/convective (usually abbreviated to convective) heat transfer coefficient between elements i and (i + 1) [$W/(m^2 * K)$].

Assuming that the thermal resistance of the glazings can be neglected, and that each surface in the window system possesses diffuse gray properties in the long-wave (3 m to 30 m) radiation region, it is possible to write a set of linear equations which can be solved for the temperature of each glazing, $TEMP_i$, and the heat transfer rate between the elements, q_i'', q''_{3a}, q''_{a4} and q''_{r34}. An energy balance applied at each glazing yields the following three equations:

$$q''_1 + (SOURCS_2) = q_2'' \tag{3.3}$$

$$q_2'' + (SOURCS_3 - q''_{3a}) = q''_{r34} \tag{3.4}$$

$$q''_{r34} + (SOURCS_4 + q''_{a4}) = q''_4 \tag{3.5}$$

where

$$q''_i = JU_i - JD_{i+1} + \hat{h}_i * (EB_i - EB_{i+1}), \tag{3.6}$$

$$JU_i = EU_i * EB_i + RU_i * JD_{i+1} + (1 - ED_i - RD_i) * JU_{i-1}, \tag{3.7}$$

$$JD_i = ED_i * EB_i + RD_i * JU_{i-1} + (1 - EU_i - RU_i) * JD_{i+1}, \tag{3.8}$$

$$\hat{h}_i = h_i * (TEMP_i - TEMP_{i+1})/(EB_i - EB_{i+1}), \tag{3.9}$$

$$EB_i = \sigma * TEMP_i^4, \tag{3.10}$$

and σ is the Stefan-Boltzmann constant ($5.669 * 10^{-8}/(m^2 * K^4)$). To model the indoor and outdoor surroundings as the 1st and 5th elements of the window system, Equations 3.7 and 3.8 are modified slightly. The inner and outer surfaces are modeled as small surfaces in large enclosures. It is assumed that the amount of radiation which leaves

these glazings and is reflected back to the glazings by the surroundings is negligible. Treating the indoor environment as a black cavity,

$$JU_1 = EB_1 \tag{3.11}$$

The radiosity of the outdoor environment is expressed as

$$JD_5 = ED_5 * EB_5 \tag{3.12}$$

where

$$ED_5 = F_{sky} * F_c * E_{sky} + (1 - F_{sky} * F_c), \tag{3.13}$$

F_{sky} is the window-to-sky shape factor (0.5),

F_c is the fraction of sky which is clear [-],

E_{sky} is the clear-sky emittance $(R_{sky}/(\sigma * TEMP_5^4))$,

and R_{sky} is the long-wave sky radiation falling on a horizontal surface $(5.31 * 10^{-13} * TEMP_5^6 \ W/m^2)$.

Convective heat transfer coefficients, h_i, for air are related to the Nusselt number, Nu_i by the equation

$$h_i = Nu_i * k/TAS_i \tag{3.14}$$

where k is the thermal conductivity of the air [W/(m * K)]. The following correlations are used to calculate the Nusselt number in the vertical interpane air space:

$$Nu_2 = [Nu_a, \ Nu_b, Nu_c]_{max} \tag{3.15a}$$

where

$$Nu_a = 0.0605 * Ra_2^{1/3}, \tag{3.15b}$$

$$Nu_b = [1 + [(0.104 * Ra_2^{0.293}/(1 + 6310/Ra_2)^{1.36})]^3]^{1/3}, \tag{3.15c}$$

$$Nu_c = 0.242 * (Ra_2/A_2)^{0.272}. \tag{3.15d}$$

Assuming that air is an ideal gas (having a compressibility factor of 1), the Rayleigh number of air space 2, Ra_2, is calculated as follows:

$$Ra_2 = (g * \beta * \Delta T * TAS_2)/(\nu * \alpha) \tag{3.16}$$

where g is the gravitational acceleration $[m/s^2]$,

β is the expansion coefficient of air [1/K] and is calculated as $1/T_{m,2}$ where $T_{m,2}$ is the mean temperature of air layer 2 [K],

ΔT is the temperature difference across the air gap [K],

and ν is the kinematic viscosity of the air [m^2/s].

The aspect ratio, A_2, is calculated as

$$A_2 = HGHT/TAS_2 \tag{3.17}$$

where HGHT is the window height [m]. The physical properties of the air are evaluated at the mean temperature of the air layer, $T_{m,2}$, which is calculated as

$$T_{m,2} = (TEMP_2 + TEMP_3)/2. \tag{3.18}$$

The indoor convective film coefficient, h_1, for a vertical window is set equal to 3.04 $W/(m^2 * K)$.

The outdoor convective film coefficient, h_4[$W/(m^2 * K)$], on a window facing a windward direction is calculated as

$$h_4 = 8.07 * V^{0.605} \quad \text{for } V \geq 2 \text{ m/s, or} \tag{3.19a}$$

$$h_4 = 12.27 \quad \text{for } V < 2 \text{ m/s} \tag{3.19b}$$

where V is the wind speed [m/s]. If the window is facing a leeward direction, then

$$h_4 = 18.64\ (0.3 + 0.05 * V)^{0.605}. \tag{3.20}$$

In the VISION program, an iterative procedure is used to solve for the glazing temperatures and heat flows using Equations 3.3 through 3.10. Initial guesses are made for the glazing temperatures, $TEMP_i^{OLD}$, and corresponding values of EB_i and $\hat{h}_i$ are calculated. A system of simultaneous linear equations in JU_i, JD_i and EB_i is solved and from the solution, updated glazing temperatures, $TEMP_i^{NEW}$, and heat flows, q_i'', are obtained. This procedure is repeated until the glazing temperatures have converged to within a specified tolerance. This method was used in

the present analyses, with the conductive/convective heat transfer between the glazings and the laminar air flow layer, q_{3a}" an q_{a4}", being accounted for in the heat source terms in Equations 3.4 and 3.5, the radiative heat transfer between glazings 3 and 4 being indicated as q_{r34}" and the convective heat transfer coefficient between these glazings, h_3, being set equal to zero. This method is similar to that proposed by Wright [23]. Calculation of the q_{3a}" and q_{a4}" terms is discussed in Sections 3.3.1 and 3.4.1.

3.3 Simplified Computer Modeling to Predict The Thermal Performance of the LAFSW

3.3.1 Description of the Slug Flow Model

As a first approximation, readily obtainable solutions for physical situations close to the situation of interest were used to predict the heat transfer through the laminar air flow layer. Since the objective of the analysis was to investigate developing flow between parallel plates, the actual temperature field was expected to lie between that for slug flow (i.e. constant velocity flow) and that for fully developed laminar flow. Also, the temperature field solution was expected to be bounded by those for constant inside wall temperature and constant wall heat flux boundary conditions. Therefore, as a first approximation, the solution for the temperature field in the laminar air flow layer is bracketed by solutions for the following flow types and boundary conditions:

1) slug flow with constant heat flux at the inside surface;
2) slug flow with constant temperature at the inside surface;
3) fully developed flow with constant heat flux wall conditions;
4) fully developed flow with constant temperature at the inside surface.

Analytical solutions were developed for the slug flow cases. A solution for the fully developed flow case with constant wall temperature was

found in the literature (21). No solution was found for the case of fully developed flow with constant heat flux at the wall.

Since there is convection and radiation on the outer surfaces of the glazings bounding the laminar air flow gap, temperature gradients exist along these glazings. Thus, the constant heat flux wall condition was expected to give more accurate solutions.

For slug flow, u = U (the uniform inlet velocity) and v = 0 everywhere. Therefore Equation 3.2 reduces to

$$U(\partial T/\partial x) = \alpha(\partial^2 T/\partial y^2) \qquad (3.21)$$

Solutions of Equation 3.21 were found for the boundary conditions of

a) constant wall temperature on both walls,
b) constant wall temperature on one wall, constant heat flux on the other wall,

as shown in Figure 3.2.

Temperature Field, Constant Heat Flux at Inside Surface

Non-dimensional distances x* and y*, and non-dimensional temperature, * , are defined as follows:

$$x^* = x/(L^*Re^*Pr) \qquad (3.22)$$

$$y^* = y/L \qquad (3.23)$$

$$\Theta = (T(x,y) - T_o)/(q''_L{}^*L/k) \qquad (3.24)$$

where x,y = distances from the origin in x and y directions respectively, [m],
L = width of channel [m],
Re = Reynolds number [-],
Pr = Prandtl number [-],

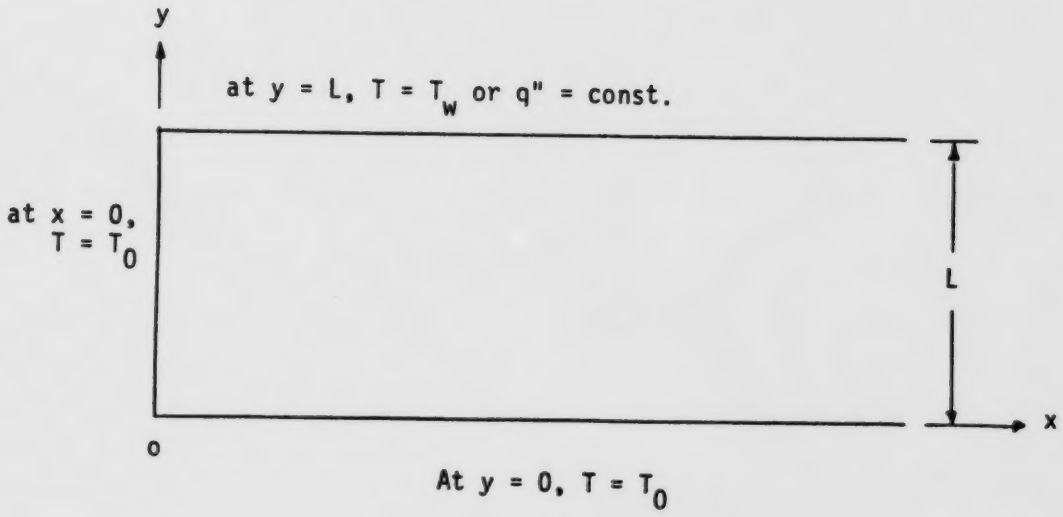

Figure 3.2 Diagram of boundary conditions for slug flow airflow model

$T(x,y)$ = temperature within the channel [K],

T_o = constant wall temperature at x=0 or y=0 [K],

q''_L = constant boundary heat flux at y=L [W/m^2],

and k = thermal conductivity of the fluid [$W/(m^2 * °K)$].

Solving Equation 3.21 using the method of separation of variables subject to these boundary conditions gives the following:

$$\Theta(x^*,y^*) = y^* + \sum_{n=1,3,5}^{\infty} (-8/(n\pi)^2)\sin((n\pi)/2)e^{(-x^*(n\pi)^2/4)}\sin(n\pi y^*/2) \tag{3.25}$$

and

$$(\partial\Theta/\partial y^*) = 1 + \sum_{n=1,3,5}^{\infty} -(4/n\pi)\sin(n\pi/2)e^{(-x^*(n\pi)^2/4)}\cos((n\pi y^*)/2) \tag{3.26}$$

Temperature Field, Constant Temperature at Inside Surface

For this set of boundary conditions, the non-dimensional temperature, ψ, is defined as

$$\psi = [T(x,y) - T_o]/[T_w - T_o] \tag{3.27}$$

where T_w = constant wall temperature at y=L [K].

The non-dimensional temperature field is

$$\psi(x^*,y^*) = y^* + \sum_{n=1}^{\infty} (2/n\pi)\cos(n\pi)e^{(-x^*(n\pi)^2)}\sin(n\pi y^*) \tag{3.28}$$

and

$$(\partial\psi/\partial y^*)\Big|_{y^*=0} = 1 + \sum_{n=1}^{\infty} 2\cos(n\pi)e^{(-x^*(n\pi)^2)}\cos(n\pi y^*) \tag{3.29}$$

The primary purpose for obtaining these solutions was to determine the amount of heat that passes through the supply air layer. A second purpose was to assess the effect of flow development on the heat transfer. To compare the solutions for the slug flow and fully

developed cases, the local Nusselt number (Nu_x) at each plate for each solution was determined.

Nusselt Number, Constant Heat Flux at Inside Surface

For internal flow, the local Nusselt Number Nu_x is defined as:

$$Nu_x = (h_x/k)L \tag{3.30}$$

where h_x = local convection heat transfer coefficient [$W/(m^2 * K)$].

From the definition of convection heat coefficient

$$h_x = (q")/(T_s - \bar{T}) \tag{3.31}$$

where $q"$ = local heat flux at wall [W/m^2], at $y = 0$,
T_s = temperature of wall in contact with fluid [K],
and T = local bulk fluid temperature [K].

Solving Equation 3.24 for T(x,y) yields

$$T(x,y) = \Theta(q"_L * L/k) + T_o \tag{3.32}$$

Substituting Equation 3.32 into 3.31 gives:

$$h_x = [q"/(\Theta_s(q"_L * L/k) - \bar{\Theta}(q"_L * L/k))] = (k/L(\Theta_s - \bar{\Theta})) * (q"/q"_L) \tag{3.33}$$

Substitution of Equation 3.33 into 3.30 yields:

$$Nu_x = (q"/q"_L)/(\Theta_s - \bar{\Theta}) \tag{3.34}$$

At the $y = 0$ surface, $q"/q"_L = -\partial\Theta/\partial y^*\Big|_{y=0}$ and $\Theta_s = 0$, so therefore

$$Nu_x\Big|_{y=0} = (\partial\Theta/\partial y^*)\Big|_{y=0} \; /\bar{\Theta} \tag{3.35}$$

At the y = L surface, $q'' = q''_L$ and $\Theta_s = \Theta_L$, so therefore

$$Nu_x \Big|_{y = L} = 1/(\Theta_L - \bar{\Theta}) \tag{3.36}$$

The local bulk fluid temperature for the constant wall heat flux boundary condition, $\bar{\Theta}$, is calculated as

$$\bar{\Theta} = \int_0^1 \Theta \, dy^* = 1/2 - \sum_{n=1,3,5}^{\infty} (16/(n\pi)^3) \sin(n\pi/2) \, e^{(-x^*(n\pi)^2/4)} \tag{3.37}$$

Nusselt Number, Constant Temperature at the Inside Surface

Using an analysis similar to that used to derive Equations 3.35 and 3.36, the local Nusselt numbers at each plate for the constant temperature boundary condition can be expressed as

$$Nu_x \Big|_{y=L} = (\partial\psi/\partial y^*)\Big|_{y^*=1} / (1 - \bar{\psi}) \tag{3.38}$$

and

$$Nu_x \Big|_{y=0} = (\partial\psi/\partial y^*)_{y^*=0} / \bar{\psi} \tag{3.39}$$

The local bulk fluid temperatures for the constant wall temperature boundary condition, $\bar{\psi}$, is calculated as

$$\bar{\psi} = \int_0^1 \psi \, dy^* = 1/2 + \sum_{n=1}^{\infty} (-2/(n\pi)^2)(1 - \cos(n\pi)) e^{(-x^*(n\pi)^2/4)} \tag{3.40}$$

3.3.2 Comparison of the Ratio of Fluxes at y = 0 and y = L Plates

Evaluation of the effectiveness of the LAFSW in reducing conductive heat transmission was made by determining the ratio of the

mean flux exiting the airflow through the exterior plate to the mean flux entering through the adjacent plate (q''/q''_L). For an ordinary window in the absence of solar radiation, this ratio would be unity for any length of window. For a LAFSW, this ratio would vary along the length of the window, as shown in Table 3.1. Modeling the laminar supply air flow as slug flow, this heat flux ratio is lower for the constant flux case than for the constant temperature case, as would be expected.

3.3.3 Comparison of Local Nusselt Numbers

Slug Flow, Constant Temperature or Constant Heat Flux at Inside Surface

Local Nusselt numbers were calculated for y = 0 and y = L plates for both the constant temperature and constant flux cases in slug flow. They are plotted in Figure 3.3.

The local Nusselt numbers at the y = L plate are higher for the constant flux case, particularly at the entrance. This occurs because for the constant heat flux case

$$Nu_{x \quad y=L} = 1/(\theta_L - \bar{\theta})$$

and at the entrance the difference $\theta_L - \bar{\theta}$ is very small. For a similar reason, the value of Nu_x at the y = 0 plate is also higher for the constant heat flux case.

As x* approaches infinity, Nu_x approaches values of 2 and -2 for the y = L and y = 0 plates respectively, as expected. At large x, the temperature distribution becomes linear, as shown in Figure 3.3(a). For the constant inside wall temperature boundary conditions

$$h_x\Big|_{y=L} = \left\{q''_L/(\psi_L - \bar{\psi})\right\}(T_w - T_o) \qquad (3.41)$$

and

$$q''_L = -k(\partial\psi/\partial y^*)_{y=L}\,[T_w - T_o] = k\psi_L/L(T_w - T_o) \qquad (3.42)$$

Table 3.1

Flux Ratios, Constant Temperature and Constant Flux

x*	Flux Ratio - Constant Temperature	Flux Ratio - Constant Flux
0.00	0.0000	0.0000
0.01	0.0000	0.0000
0.02	0.0000	0.0000
0.03	0.0000	0.0000
0.04	0.0003	0.0001
0.05	0.0013	0.0004
0.06	0.0033	0.0013
0.07	0.0066	0.0027
0.08	0.0112	0.0049
0.09	0.0171	0.0078
0.11	0.0250	0.0114
0.12	0.0332	0.0157
0.13	0.0422	0.0206
0.14	0.0519	0.0260
0.15	0.0622	0.0319
0.16	0.0279	0.0333
0.17	0.0840	0.0449
0.18	0.0953	0.0519
0.19	0.1068	0.0592
0.20	0.1184	0.0666

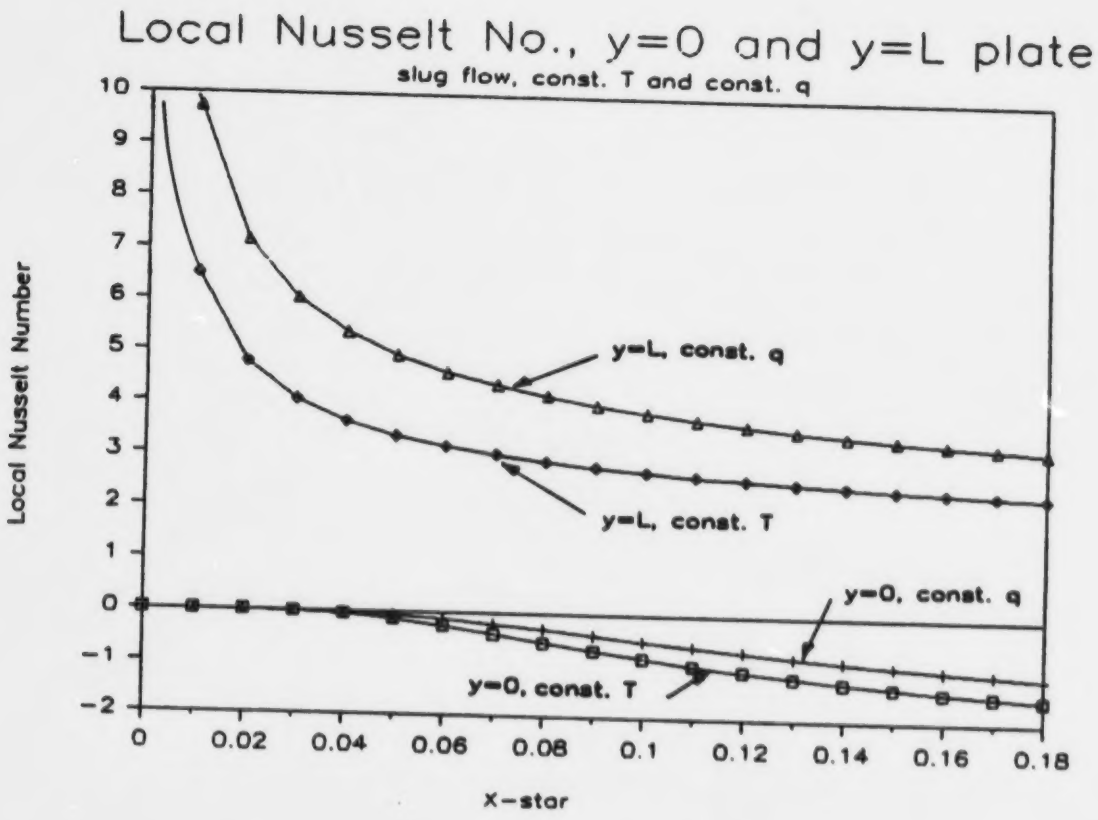

Figure 3.3 Local Nusselt numbers at the y=0 and y=1 plate, for the slug flow case with either constant temperature or constant heat flux boundary conditions.

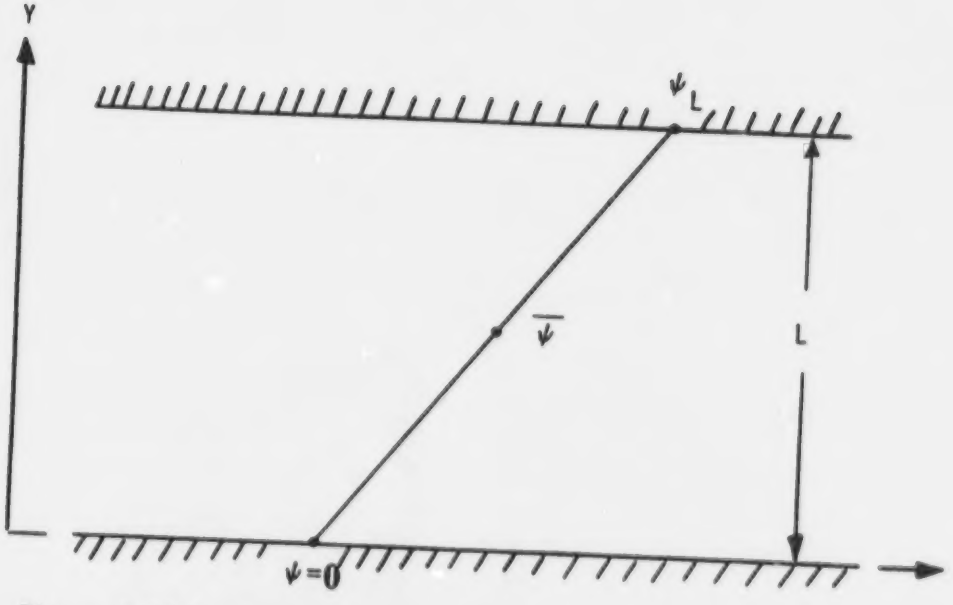

Figure 3.3(a) Temperature distribution for infinite plates with slug flow at large x^*, for constant temperature conditions at the $y = L$ plate

$$h_x = [(k\psi_L)/L]/[\psi_L - \overline{\psi}] \qquad (3.43)$$

For a linear temperature profile,

$$\overline{\psi} = \psi_L/2. \qquad (3.44)$$

Substituting Equation 3.44 into 3.43:

$$h_x = k\psi_L/L(\psi_L/2) = 2k/L \qquad (3.45)$$

Since $Nu_x = h_xL/k$,

$$Nu_x = (2k/L)(L/k) = 2. \qquad (3.46)$$

So $Nu_x = 2$ at the $y = L$ plate. Similarly, $Nu_x = -2$ at the $y = 0$ plate, since $\psi_0 - \psi = -\psi_L/2$.

For the constant flux case, the above analysis is also valid because the heat flux at the cold plate will match that of the hot plate at large x.

While on a percentage basis, the Nusselt values for the $y = L$ wall differ significantly between the constant temperature and constant flux cases, they are both in the same order of magnitude.

Slug and Fully Developed Flow, Constant Temperature

Hatton and Turton (21) developed relations for the local Nusselt number along two plates for fully developed flow, with constant unequal temperatures at each wall. Their results could not be used directly since their definition of Nu_x is greater by a factor of 2 and -2 at the $y = L$ and $y = 0$ walls respectively. However, their results were transformed to the present definition of Nu_x and are and plotted against Nu_x for slug flow, constant temperature in Figure 3.4.

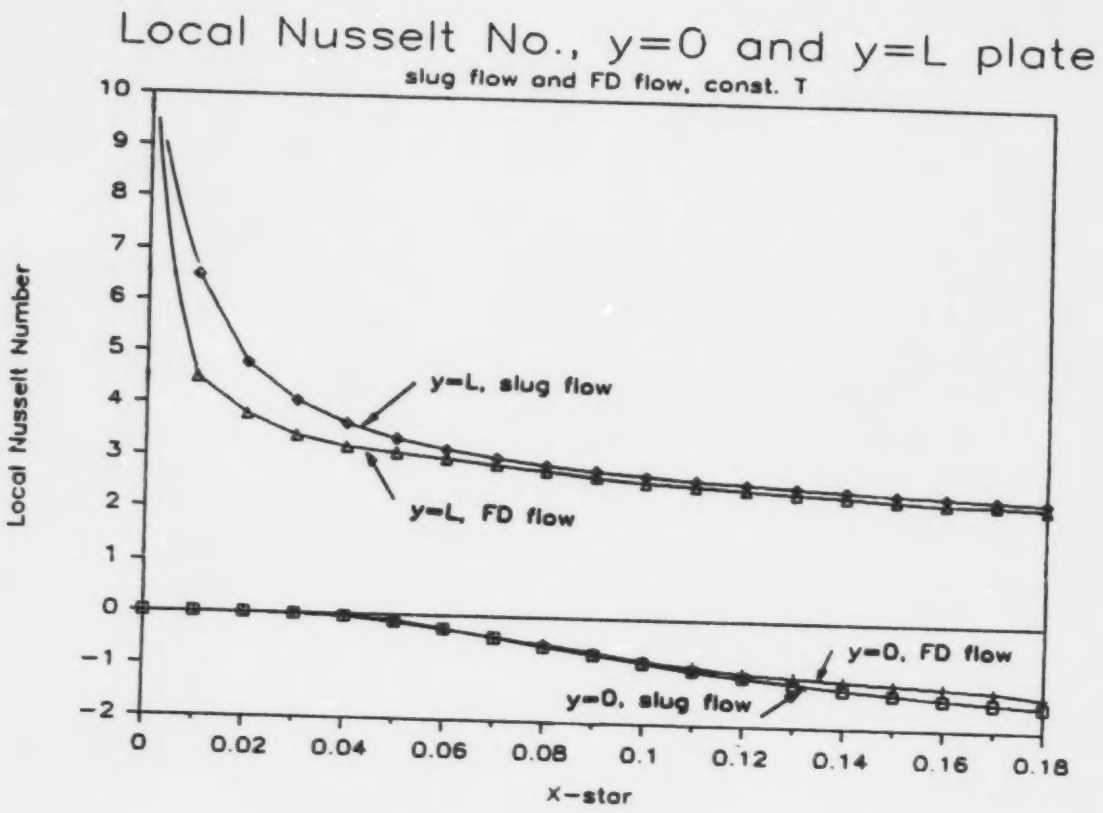

Figure 3.4 Local Nusselt numbers at the y=0 and y=L plate, for both the slug flow and the fully developed air flow conditions.

The values of Nu_x compare quite closely for the two cases, with Nu_x for the fully developed flow being slightly lower near the entrance for the y = L plate, and infinitely high at the entrance. This is because the Nusselt number is proportional to $\partial T/\partial x$ and $1/\Theta$. Referring to Equation 3.21, $\partial T/\partial x$ is inversely proportional to the freestream velocity, U. At each wall u is very low, making $\partial T/\partial x$ higher than that for slug flow, increasing Nu_x. After a short distance from the entrance, Nu_x would be smaller than that for slug flow, since the bulk fluid temperature, Θ, would be higher for fully developed flow.

3.3.4 Window Dimensions

Before a computer simulation to evaluate the performance of the LAFSW could be done, there remained the problem of the determining dimensions of the window. Tjelflaat and Bergesen (22) state that for fully developed channel flow between walls at differing temperatures, the ratio Gr/Re must be less than 24 to avoid hydrodynamic instability.

It was decided to choose x*, the non-dimensional length of the window so that the ratio of the mean conductive flux passing through the outer plate to that passing through the inner plate was approximately 1%, i.e., only 1% of the heat entering the inner pane due to conduction would pass out of the outer pane. For the constant heat flux case, with slug flow, this occurs at x* = 0.1.

Since Re is proportional to L, the spacing between plates, and Gr is proportional to L^3, there is a practical limit to L, since x* should not exceed 0.1. The height of the window, x, was to be a practical height of approximately 1 meter.

By a trial-and-error technique, L was fixed at .0127 m and Re = 1000. This meant that since x/(L*Re*Pr) = .1, with Re = 1000, Pr = 0.72 for air, and L = .0127, x would be 0.91 m. A check of the Grashof number yields:

$$Gr = [g \beta (\Delta T) L^3]/\nu^2$$

$$= [9.81 \times 1/273 \times (13)] \times [(.0127)^3/(1.109 \times 10^{-5})^2]$$

$$= 7780.3$$

where g = gravitational constant [m/s^2],
β = 1/mean temperature [1/K],
T = mean temperature difference [K],
L = distance between panes [m],
and ν = kinematic viscosity of air [m^2/s].

Then Gr/Re = 7780/1000 = 7.78, which is less than 24, so hydrodynamic stability is assured.

With the Reynolds number fixed at 1000, the air velocity $u = \nu Re/L = (1.109 \times 10^{-5})(1000)/(0.0127) = 0.873$ m/s.

The one dimension remaining is the window width. Since the volumetric flowrate is directly proportional to window width, the width could be adjusted for the particular application. If the ASHRAE 62-81 requirement of 5 liters/second per room is maintained, then assuming 7 rooms in a house:

$$W = V/UL = (.005\ m^3/s \times 7)/((0.873\ m/s)(0.0127\ m)$$

$$= 3.157\ m$$

where W = window width [m],
V = volumetric flowrate [m^3/s],
u = air velocity [m/s],
and L = window gap width [m].

The window would be 3.2 m wide.

3.3.5 Window Performance Simulation

3.3.5.1 Approach

With the dimensions of the window determined and a means developed to find heat transfer across the air flow gap, the approximate evaluation of window performance was done. To evaluate the thermal performance of the window, a set of algorithms based on those in the VISION computer program [9] were used. VISION was modified by Wright to allow the simulation of a LAFSW [10], and the same scheme, as described in Section 3.2, was used here. The principal difference between our method of modeling air flow in this approximate approach and that of Reference 10 is that we modeled the airflow as slug flow, and used a constant heat flux wall condition, and in Reference 10 the flow is modeled as fully developed flow with a constant temperature wall condition.

3.3.5.2 Window Performance without Solar Radiation

Three cases of the LAFSW were modeled; the baseline case, with airflow between the middle and outer pane of a triple glazed window in the absence of solar radiation, and the same window system with low emittance coatings applied to either the outer or inner surface of the middle glazing. A higher emittance value is given to a coating on the supply-air side of the glass to reflect the different properties of the more durable coating that would have to be used.

Results are found in Table 3.2. Note the substantial decrease in U-value that results with air flow, particularly when low emittance coatings are used.

3.3.5.3 Window Performance with Solar Radiation

To evaluate daytime window performance, the window was modeled with incident solar radiation. The window tested was a triple-glazed unit with a low emittance coating on the outer surface of the middle pane, Case 5 in Table 3.2. This glazing had normal optical properties of 0.60 normal transmittance, 0.25 reflectance for solar radiation incident on the coating side and a reflectance of 0.22 on the substrate side.

The absorption of solar radiation in each window pane was calculated for Winnipeg (49°N latitude, 97°W longitude) at 11:30 a.m. local standard time on February 21, with an incident beam radiation on a south-facing vertical window of 727.97 W/m^2 and incident diffuse radiation of 109.28 W/m^2. Optical properties of the glazings were calculated using the technique found in the 1985 ASHRAE Fundamentals, Chapter 27. Simulations were performed for both this case and a case where the incident angle of radiation was the same, but the radiation was reduced to a third of the first case. Glazing temperatures and the mean temperature of the exiting supply air were determined for inside and outside temperatures of 21°C and -18°C respectively.

The mean air temperature of the supply air in the first case was 263.78 K (-9.37°C) for an increase of 8.63 °C. The exit air temperature in the second case was 260.73 K (-12.42 °C). One possible application of preheated supply air would be as a defrosting mechanism for an air-to-air heat exchanger. The defrosting effect would not be continuous, but intermittent in periods of higher temperatures, and when sunlight strikes the panes, increasing the supply air temperature. Using the supply air for defrosting the heat exchanger would not only reduce the energy input for defrosting, but it would probably eliminate the need for the defroster hardware.

To achieve defrosting, the supply air temperature must be at the freezing point or higher. Therefore, warmer supply air temperatures would be required. A lower ratio between entering and exiting fluxes in the air stream would be accepted if the supply air temperature could be increased. The temperature could only be increased by altering the window plate spacing, the plate height, or air velocity; however, alteration of these parameters, as it was noted before, could result in hydrodynamic instabilities in the air flow.

Previously, the Gr/Re ratio was kept at 7.78. To maintain the same degree of stability, this ratio was retained. But Gr/Re is proportional to L^2/U, the ratio of the square of the plate spacing and the fluid velocity. If this ratio was kept constant, then so would the

Gr/Re ratio. The velocity was halved, so the plate spacing was reduced by $2^{1/2}$.

Then $L = 0.0127/1.4 = 0.009$ m

$U = 0.874/2 = 0.437$ m/s

$m = 1/(2 \times 1.414)\ m_{old} = 0.3536\ m_{old}$

where L = plate spacing [m],

u = air velocity [m/sec],

and m = mass flowrate of air [kg/s].

Using these values, Re = 354. If x, the height of the window, remained 0.91 meters high, then

$$x^* = x/(LRePr) = 0.91/[(0.009(354)(0.72)] = 0.396$$

The flux ratio for this air flow is 0.0322, or approximately 3%, as compared to approximately 1% for the original dimensions. The mean temperature of the exiting air should increase significantly. To maintain the same volume of air flow for the house described previously, the window width would have to be increased to 8.9 m.

As will be shown by the exact analysis in the next section, reducing the air flow in this way, to increase the outlet temperature, sharply reduces the thermal resistance of the LAFSW. In the case of a window with a low-E coating on the outside of the middle pane, the thermal resistance decreased from RSI = 2.5 m^2K/W to RSI = 1 m^2K/W. Fortunately, the humidity controlled air inlet system which is recommended for use with the LAFSW allows the higher flow rates to be used, so that the higher thermal resistances calculated in this section can be considered attainable.

A competing super window might be based on a low-E coating coupled with a low conductance gas fill. To compare this approach with the LAFSW, a window with the laminar air flow between the middle and outer panes replaced by an absolute vacuum was analyzed. The properties of this window were as in Case 5, Table 3.2. The thermal resistance of

this window was only 40% of that of the LAFSW. At first glance, this result might appear amazing, since an absolute vacuum completely eliminates convective heat loss between panes. However, an inspection of the pane temperatures explains this result. The middle pane of the LAFSW is at 264.8 °K (-8.35°C), because it is cooled by the laminar air flow over it. The middle pane of the evacuated window is at 282.45 °K (9.3°C). Thus the radiation loss across the laminar flow air space is far less than that across the evacuated space.

The thermal resistance of a window is not constant. It depends on ambient conditions. This is particularly true of the LAFSW, because of the fact that radiation is the dominant heat loss mechanism. The cases analyzed above had an outdoor temperature of -18°C and a clear night sky. The outer pane in Case 5 was almost 2°C below the ambient temperature, so that it actually gained heat from the outdoor air. The only heat loss mechanism was radiation to the night sky. Obviously a thermal resistance based on the indoor outdoor temperature difference has little meaning in such a case. The thermal resistance of this window would be increased by windy weather! It would be very sharply increased by cloudy weather. It would also be increased by a higher ambient temperature, since radiation varies with the fourth power of the temperature.

This means that the thermal resistance values quoted here should be considered to apply only to these specific conditions. An annual average value would require an hour-by-hour analysis which is beyond the scope of the present project. However, the conditions chosen for this study are conservative, and the annual average thermal resistance would be expected to be substantially higher than the values quoted above.

3.4 Detailed Computer Modeling to Predict the Thermal Performance of the LAFSW

3.4.1 The Computer Model

In section 3.3, above, a simplified approach was described in which a solution to the heat transfer problem was found for the case of slug flow between two parallel plates of constant heat flux. This heat

transfer solution was then combined with a one-dimensional solution to the window heat transfer problem based on the approach used in VISION.

In the present section, a more exact solution to the heat transfer problem was found. This solution took into account the development of the flow as well as the heat transfer. It also dealt with the varying boundary conditions which could be characterized as "constant temperature" or "constant heat flux." To accurately solve this complex heat transfer problem, a computer program, called LAMWIN, was developed. This program was developed to evaluate in detail the performance of the window and to investigate the effect of different design parameters on the performance of the window.

Since the velocity profile in the laminar air flow gap is in the developing stage, the local conductive/convective heat transfer coefficient varies along the window panes. Combined with the increased bulk temperature of the air in the laminar air flow gap along the panes, this causes temperature gradients to exist along the middle and outer glazings. Due to the long-wave radiative heat transfer between these glazings and the inner glazing, a temperature gradient also exists along the inner pane. To solve for the temperature distribution along the glazings, the local heat transfer rates, and the corresponding overall thermal performance of the window, the window system was divided into a network of nodes, as shown in Figure 3.5. Assuming that the thermal resistance of the glazings is negligible, each window pane was subdivided by a set of nodes running in the x-coordinate direction. To allow for modeling of the velocity and temperature profiles in the laminar air flow gap, this layer was subdivided using a two-dimensional finite-difference mesh lying in the xy plane shown in Figure 3.5.

A literature review revealed that the problem of determining the velocity distribution in a fluid flowing between parallel plates and undergoing development from an initial profile at the inlet to a fully developed profile for downstream had been solved by several researchers. In the present problem, the temperature of the air in the laminar air flow layer is within a relatively narrow range, and therefore the

Table 3.2

Window performances of the LAFSW with slug flow, with and without low emissivity coatings, compared to a simple triple glazed window

Case	T_o (°K)	E_{outer} (-)	E_{inner} (-)	Exit Air Temp(°K)	U-value (W/m^2°K)	Comments
1	284.98	0.84	0.84	--	1.85	Simple triple glazed window, no airflow
2	281.84	0.84	0.84	258.79	0.696	Triple glazed unit, airflow with constant flux center glazing
3	281.22	0.84	0.84	259.00	0.793	Above with constant temperature center glazing
4	286.53	0.84	0.09	257.41	0.476	Case 2 above, low E film on inner surface of center pane
5	282.26	0.35	0.84	259.26	0.390	Case 2 above, hard coat low E coating on outer surface of center pane

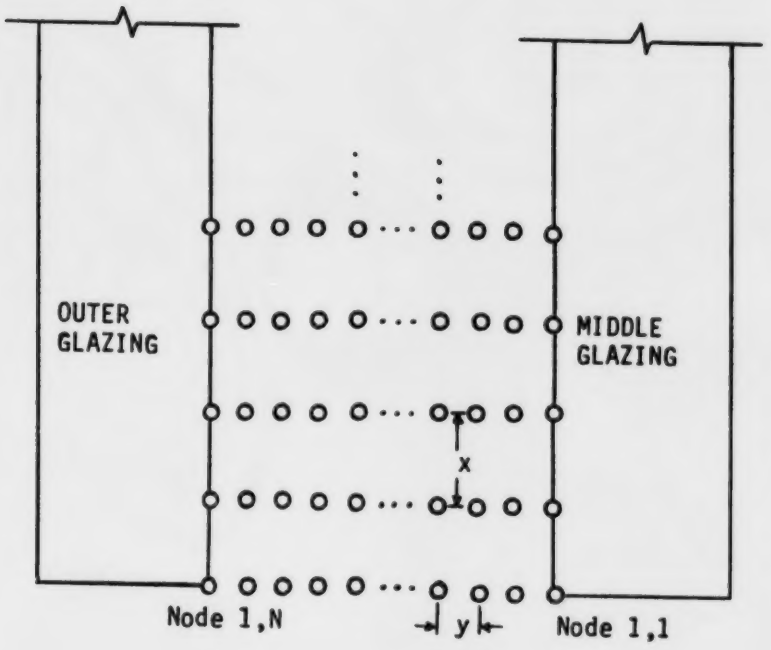

Figure 3.5 Finite Difference Grid Network in the Laminar Air Flow Gap

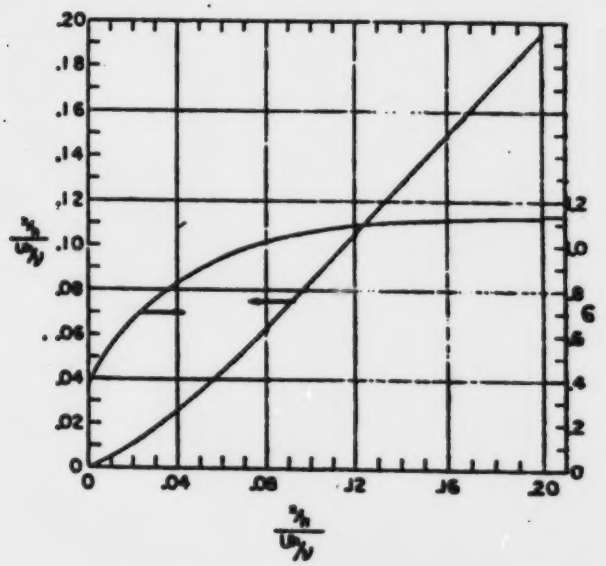

Figure 3.6 Relationships between the physical coordinate, x, the stretched coordinate, $\hat{x}$, the stretching factor, ϵ, for flow between parallel plates (from Reference 24)

physical properties of the air were assumed to be constant. An explicit equation describing the u-component velocity profile of a fluid with constant properties flowing between parallel plates was developed by Sparrow, Lin and Lundgren [24]. For the coordinate system shown in Figure 3.5 the non-dimensional u-component of velocity in the region $0 \leq Y \leq 1$ is given by

$$(u/U) = 1.5(1/(1-Y)^2) + \sum_{i=1}^{\infty} (2/\alpha_i^2)[(\cos(\alpha_i(1-Y))/\cos\alpha_i) - 1]e^{-\alpha_i^2 \hat{X}} \quad (3.47)$$

where the eigenvalues, α_i, are roots of

$$\tan \alpha_i = \alpha_i,$$

and the remaining symbols are defined as follows:

$$Y = y/a$$

$$X = x/(a * Re_a)$$

$$\hat{X} = \hat{x}/(a * Re_a)$$

where a is the half-spacing between the plates [m],

U is the u-component of the parallel and uniform velocity profile at the plate inlet [m/s],

Re_a is the Reynolds number based on the half spacing of the plates [-],

and $\hat{x}$ is a stretched coordinate [m].

Substituting Equation 3.47 into the continuity equation

$$(\partial u/\partial x) + (\partial v/\partial y) = 0 \quad (3.48)$$

and solving for v yields the following expression for the determination of the v-component of velocity in the region $0 \leq Y \leq 1$:

$$(v/V) = (1/Re_a)(2/\epsilon)\sum_{i=1}^{\infty} [(\sin(\alpha_i(1-Y))/\alpha_i\cos\alpha_i) - (1-Y)]e^{-\alpha_i^2 \hat{X}} \quad (3.49)$$

where ϵ is a stretching factor [-]. Since constant fluid properties have been assumed in the modeling of the laminar air flow layer, the velocity profiles are symmetric about the centerline of the parallel plates, i.e. the u component at (2 - Y) is equal to the u component at Y and the v component at (2 - Y) is negative the value at Y.

The relationship between the non dimensional physical coordinate X and the non-dimensional stretched coordinate $\hat{X}$ is shown in Figure 3.6. At X = 0.24, $\hat{X}$ = X, and the flow is essentially fully developed. Figure 3.6 also shows the relationship between X and the stretching factor ϵ. With increasing downstream distance, ϵ increases monotonically and approaches a limiting value of 1.135.

In using the stretched coordinate linearization method to solve the conservation of x momentum and continuity equations for the preceding velocity expressions, Sparrow et al. made the following two assumptions which are usually made in boundary layer problems and had generally been applied in all entrance region analyses up to that time:

(i) the static pressure is uniform across each system, i.e. $\partial P/\partial y$ is negligible;

(ii) the component $\mu(\partial^2 u/\partial x^2)$ of the streamwise shear stress is negligible relative to the component $\mu(\partial^2 u/\partial y^2)$, where μ is the absolute viscosity of the fluid [N * s/m^2].

Excellent agreement was observed between their results and those of Bodoia and Osterle, who solved similar equations using a finite difference technique [25]. Several researchers have subsequently solved the complete set of Navier-Stokes equations for the parallel plate hydrodynamic entrance problem. Morihara and Cheng [26] solved the problem for a parallel and uniform entrance velocity distribution using finite difference forms of quasilinearized steady-state, incompressible Navier-Stokes equations. Their solution predicted local maxima in the velocity profiles on both sides of the centerline near the walls. These local maxima had also been observed in the results of others who solved the complete set of Navier-Stokes equations, including Wang and Longwell

[27] and Brandt and Gillis [28]. Morihara and Cheng observed that the off-centerline maxima appear to be greatest at $Re_a = 100$ (or at $Re_{2a} = 200$ in their publication since they based the Reynolds number on the full channel width). At a Reynolds number of $Re_a = 1000$, the off-centerline bulges almost disappear and the velocity profiles approach those of the boundary layer approximation. For low Reynolds numbers (less than $Re_a = 100$), Morihara and Cheng also report significant deviations between the entrance region centerline velocities obtained in their solution and those obtained by Bodoia and Osterle. However, at $Re_a = 1000$, good agreement between the two centerline velocity distributions is observed. In the present analysis, the Reynolds number of the laminar air flow was of the order $Re_a = 1000$, and at Reynolds numbers of this magnitude, the results of Bodoia and Osterle or of Sparrow et al. show excellent agreement with the more rigorous results of Morihara and Cheng. Therefore, the solution obtained by Sparrow et al., Equations 3.47 and 3.49 and equations describing the curves on Figure 6, were used to calculate the u and v velocity components at each of the finite difference nodes in the laminar air flow layer. At the entrance to the parallel plates (at $x = 0$) the series for calculating the v component of velocity in Equation 3.49 does not converge except at the wall and the centerline. Also, at $x = 0$, the series for evaluating the u component of velocity in Equation 3.47 converges very slowly, and therefore a parallel and uniform velocity distribution, with $u/U = 1$ and $v = 0$ for $0 < Y < 2$, was directly specified at $x = 0$. This was the boundary condition used at the parallel plate inlet in the analysis of Sparrow et al.

In addition to those which have already been discussed, the following two assumptions were made in the LAMWIN computer model of the LAFSW:

(i) heat conduction along the glazings has a negligible effect on the overall performance of the window;

(ii) the view factor between each side of a glazing node and the node opposing it in the y direction is 1.0. In other words, it is assumed that each side of a glazing node views an entire

pane at the temperature of the opposing glazing node and that the temperature gradients along the glazings have a negligible effect on the overall radiation exchange between the glazings.

The validity of these two assumptions was verified and is discussed in Section 3.4.2. As a result of these two assumptions, the laminar air flow temperature profile and the glazing temperatures at a given streamwise location, x, depend only on the upstream conditions in the laminar air flow layer. Therefore, the LAMWIN program steps up the window height and uses forward difference forms of Equations 3.2 to predict the temperatures across the laminar air flow layer at each set of streamwise nodes, and then uses VISION heat balance Equations 3.3 through 3.10 to iteratively solve for the corresponding glazing temperatures at each streamwise location.

Using a forward difference to approximate the partial derivative $\partial T/\partial x$ in Equation 3.2 at node (m - 1,n) yields the following:

$$u_{m-1,n} \frac{T_{m,n} - T_{m-1,n}}{\Delta x} + v_{m-1,n} \left.\frac{\partial T}{\partial y}\right|_{m-1,n} = \alpha \left.\frac{\partial^2 T}{\partial y^2}\right|_{m-1,n} \quad (3.50a)$$

Solving for $T_{m,n}$ yields the form of the equation used in LAMWIN to solve for the temperature at node m,n in terms of the conditions at x station m - 1, which is

$$T_{m,n} = T_{m-1,n} + \frac{\Delta x}{u_{m-1,n}} \left[\alpha \left.\frac{\partial^2 T}{\partial y^2}\right|_{m-1,n} - v_{m-1,n} \left.\frac{\partial T}{\partial y}\right|_{m-1,n} \right] \quad (3.50b)$$

where

$$\left.\frac{\partial^2 T}{\partial y^2}\right|_{m-1,n} \approx \frac{T_{m-1,n+1} - 2\,T_{m-1,n} + T_{m-1,n-1}}{(\Delta y)^2} \quad (3.51)$$

and the following four-point finite-difference formulae are used to approximate the derivative $\partial T/\partial y$:

$$\left(\frac{\partial T}{\partial y}\right)_{m-1,n} \approx \frac{-T_{m-1,n+2} + 6\,T_{m-1,n+1} - 3\,T_{m-1,n} - T_{m-1,n-1}}{6\,(\Delta y)} \quad (3.52a)$$

$$\left(\frac{\partial T}{\partial y}\right)_{m-1,n} \approx \frac{2\,T_{m-1,n+1} + 3\,T_{m-1,n} - 6\,T_{m-1,n-1} + T_{m-1,n-2}}{6\,(\Delta y)} \quad (3.52b)$$

for n=N-1.

Since the thermal resistance of the glazings is neglected, the air temperatures at edges of the laminar layer, $T_{m,1}$ and $T_{m,N}$ equal to the temperature of glazings 3 and 4 at location m, $TEMP_{m,3}$ and $TEMP_{m,4}$ respectively.

The velocity of the laminar air flow right at the glazings is zero. Therefore, the conductive heat transfer rates between glazings 3 and 4 and the air layer, q''_{3a} and q''_{a4} in Equations 3.4 and 3.5, were calculated as follows:

$$q''_{3a} = (k_{air}/\Delta y)(TEMP_{m,3} - T_{m,2}); \quad (3.53)$$

$$q''_{a4} = (k_{air}/\Delta y)(T_{m,N-1} - TEMP_{m,4}). \quad (3.54)$$

In using the iterative technique described in Section 3.2 to determine the glazing temperatures at each x location, it is necessary to relax the solution of heat balance equations 3.3 through 3.10 to obtain a convergent glazing temperature solution. New glazing temperatures, $TEMP_i^{NEW}$, are calculated from the previous ones, $TEMP_i^{OLD}$, and the heat balance equation solution, $TEMP_i^{SLN}$, using

$$TEMP_i^{NEW} = TEMP_i^{OLD} + w(TEMP_i^{SLN} - TEMP_i^{OLD}), \quad (3.55)$$

where w is a relaxation factor [-]. $TEMP_i^{NEW}$ becomes $TEMP_i^{OLD}$, and the procedure is repeated until $(TEMP_i^{NEW} - TEMP_i^{OLD})/TEMP_i^{NEW}$ is less than a specified tolerance for all i. To insure that the solution has indeed been reached, w is then set equal to 1.0 and the iterations are continued until the convergence criterion is again satisfied. In the present study, a tolerance of 1×10^{-4} was specified, and w = 0.05 gave a satisfactory rate of convergence.

Once the glazing temperatures and local heat fluxes along the entire height of the window have been determined, overall performance characteristics such as average heat fluxes over the glazings, average glazing temperatures, heat picked up by the laminar flow supply air and U-values are calculated. The U-value based on the heat flux at the inside surface of the LAFSW, U_i, is given by

$$U_i = q_1''/[A * (T_1 - T_5)], \tag{3.56}$$

where A is the area of the window.

Based on the heat flux to the outdoor surroundings, the U-value, U_o, is given by

$$U_o = q_4''/[A * (T_1 - T_5)]. \tag{3.57}$$

To quantify the preheating potential of the window, the bulk temperature of the outgoing laminar flow supply air, T_b, is also calculated from the temperature and velocity profiles at the exit of the parallel window panes using the following equation:

$$T_b = \frac{\int_A TudA}{\int_A udA} \approx \frac{T_{M,1}u_{M,1}/2 + \sum_{n=2}^{N-1} T_{M,n}u_{M,n} + T_{M,N}u_{M,N}/2}{u_{M,1}/2 + \sum_{n=2}^{N-1} u_{M,n} + u_{M,N}/2} \tag{3.58}$$

Provision was made in the LAMWIN program to investigate the effect that heat conduction along the glazings has on the overall performance of the window. At each streamwise location, m, heat conduction to the node on glazing i from the adjacent nodes on that glazing is accounted for as a heat source term in Equation 3.3, 3.4 or 3.5, and is calculated as

$$q''_{cond(m,i)} = [(THG_i\ k_{glass})/D_m][(TEMP_{m+1,i} - 2TEMP_{m,i} + TEMP_{m-1,i})/\Delta x], \tag{3.59}$$

where $q''_{cond(m,i)}$ is the heat conduction per unit glazing area to glazing node (m,i) from the adjacent glazing nodes [W/m^2],

THG_i is the thickness of glazing i [m],

k_{glass} is the thermal conductivity of glass [W/(m * K)],
and D_m is the height of the nodes at location m [m].

Slightly different equations apply at the end nodes of the glazings (for m = 1 and m = M). Since upstream glazing temperatures are required to calculate the conduction term $q''_{cond(m,i)}$, a multiple pass iteration technique is utilized, wherein $q''_{cond(m,i)}$ is calculated using the glazing temperature distributions determined in the previous pass. For the initial pass, the glazing temperature distributions and overall performance parameters are calculated assuming no temperature gradients exist along the glazings from the previous pass, which is equivalent to neglecting heat conduction along the glazings. The temperature distributions determined in subsequent passes are relaxed by a factor w_c using a method identical to Equation 3.55. Iterations for the glazing temperature distributions and overall window performance continue until the heat pick up rate by the laminar flow supply air has converged to within a specified tolerance. To obtain a converging solution, a relatively small relaxation factor of $w_c = 0.02$ was necessary in the present study. The above-mentioned convergence criterion was overridden, and iterations were done until a visual inspection of the output showed that the glazing temperatures were not changing significantly from one pass to the next.

In determining the temperature and heat flux distributions along the glazings, the LAMWIN program steps along the panes, using upstream conditions to calculate the temperature profile across the laminar air flow layer at each streamwise location. As in any such forward-marching finite-difference technique, it is essential to choose a finite difference grid size which will ensure a stable solution. In the present analyses, a simple relationship which is applicable for fully-developed flow was used to check that a chosen grid size would not result in an unstable solution. It can be shown that for fully-developed channel flow, the relationship

$$[(1.5U(1 - ((N-1)/N)^2)(L/N)^2/(\alpha(HGHT/M)] \geq 2$$

must be satisfied for a stable solution of Equation 3.2,

where M is the number of grids in the x-direction,
and N is the number of grids in the y-direction.

3.4.2 Predicted Thermal Performance of LAFSW Using Detailed Computer Simulation Program

3.4.2.1 Validation of the Assumptions in the LAFSW Model

A triple-pane LAFSW with 12.5-mm (0.5-in.) thick sealed and laminar air flow spaces and 12.5-mm thick glass was used to investigate the effect of heat conduction along the glazings on the overall predicted performance of the window. The ambient outdoor temperature was set at -18°C and the ambient indoor temperature at 21°C. Nighttime simulations with no incident solar radiation, no wind, and no cloud cover were done. Almost 400 passes were made through the LAMWIN calculation routine, and the change in the glazing temperatures from one pass to the next was relaxed by a factor of $w_c = 0.02$. Near the end of this series of passes, it was observed that the glazing temperature distributions were not changing significantly, and it was concluded that the final solution had essentially been reached. Figure 3.7shows the initial and final glazing temperature distributions. The only significant change in the temperature distribution is near the entrance, but this does not significantly effect the overall performance. The bulk temperature drops from -15.037°C to -15.041°C and the overall window U-values change by less than 0.5%. Since these are insignificant errors, conduction along the glazings was neglected in subsequent simulations.

As stated in Section 3.4.1, the LAMWIN program assumes that each side of a glazing node views an entire pane at a temperature of the opposing glazing node, and that the temperature gradients along the glazings have a negligible effect on the overall net radiation exchange between the glazings. This assumption was validated by manually calculating the net radiation exchange between a node surface and the individual node surfaces which it views, and comparing this value to the

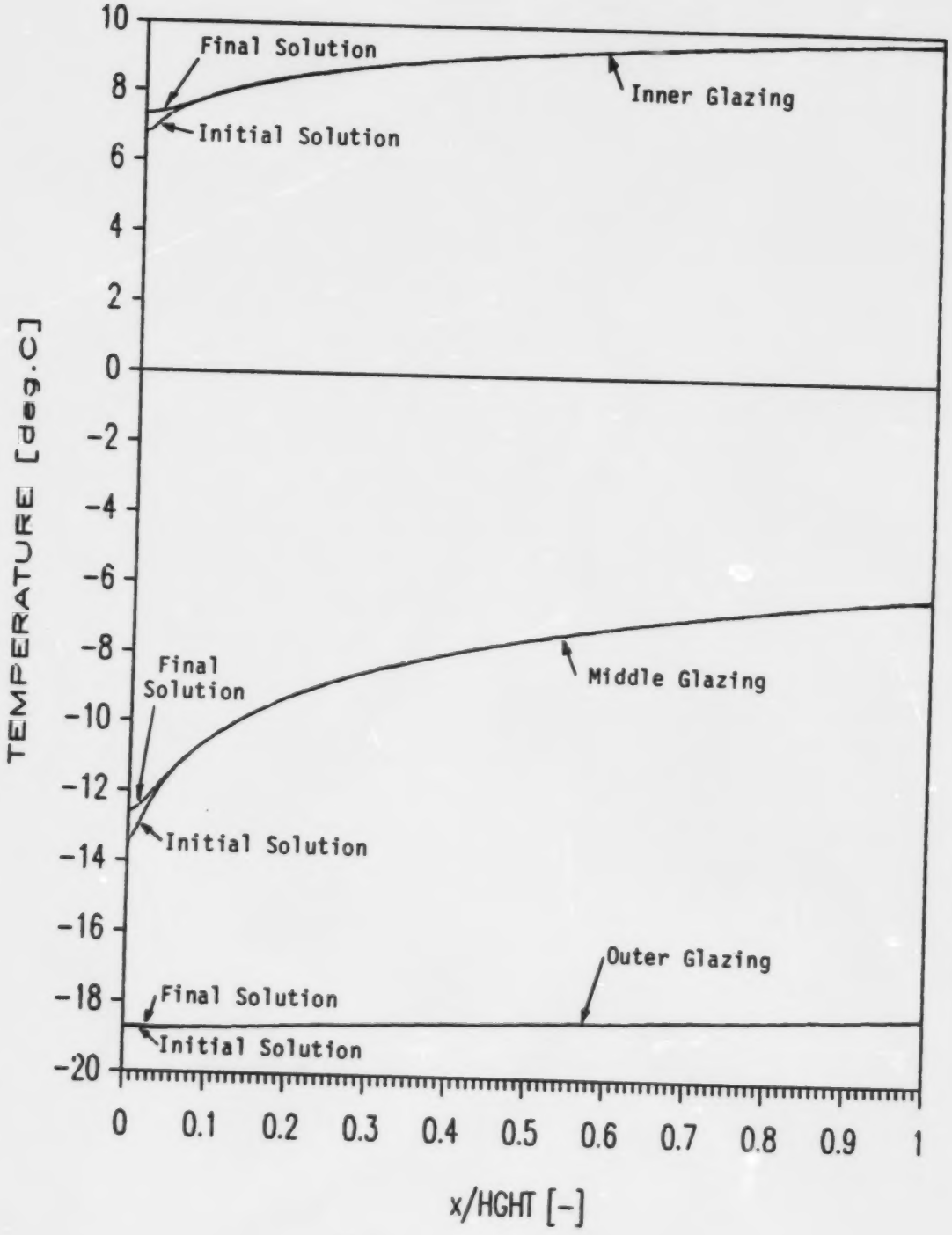

Figure 3.7 Investigation of the Effect of Heat Conduction along the Glazings

LAMWIN-calculated net radiation exchange. A region where the glazing temperature gradients were most severe was chosen for this calculation since the error would be greatest there. The error in the LAMWIN calculation was found to be less than 0.3%.

3.4.2.2 Comparison with Approximate Analysis

It was expected that the finite difference model, if free of programming errors, would predict thermal performance results close to those of the approximate analysis which had been carried out using the slug flow model. Several comparisons were made and it was found that the agreement between the overall heat transfer predictions was good. This indicated both that the finite difference model was free of errors and that the approximation of slug flow with constant heat flux walls was a good one.

On the other hand, some of the details of the results obtained using the two methods were quite different. This was particularly true of the convective heat flux at the outer pane. In the simplified model, the outer pane was assumed to be at the temperature of the incoming air. As the more detailed simulation showed, it was actually higher, because of radiant heat transfer from the middle pane. This resulted in a heat gain to the laminar air stream in the lower part of the window, turning to a loss only in the upper part of the window as the thermal boundary layer penetrated from the inner to the outer pane.

3.4.2.3 LAFSW Configuration Simulated

The LAMWIN computer program was used to simulate a number of different triple-glazed LAFSW configurations. In all cases, the ambient outdoor temperature was set at -18°C and the ambient indoor temperature at 21°C. The window was located on the windward side of a building with a wind speed of 6.67 m/s. The fraction of the sky which is cloud covered was set at 0.5. Both nighttime and daytime simulations were performed. To do daytime simulations, it was necessary to calculate the solar radiation absorption rate in each of the three panes making up the

window. ASHRAE-standard 3.175-mm (1/8-in.) thick DSA glass was specified as the glazing material, and the cosine polynomial coefficients listed in the 1985 Fundamentals Handbook for this glass type were used to calculate the beam optical properties of the individual panes [29]. The overall beam optical properties of the triple-glazed window were calculated using Edwards' embedding technique [23]. The overall diffuse optical properties of the multi-glazed system were determined by integrating the beam properties over a hemisphere using cosine polynomial coefficients describing the variation of the beam properties with incidence angle [9]. As in Section 3.3.5.3, the solar radiation absorption rates were calculated for Winnipeg at 11:30 a.m. local standard time on February 21 when the incident beam and diffuse radiation on a vertical south-facing window during a clear day are 728.0 W/m^2 and 104.3 W/m^2 respectively.

In the present analysis it was assumed that the primary application of a LAFSW will be to preheat the fresh air supply to a heat exchanger. In this application, the total supply air flow rate through all of the LAFSW in a house would have to provide the required ventilation rate. In the present analysis, it was assumed that a typical house would have approximately 10 m^2 (108 ft^2) of window area and would require 35 l/s (74 cfm) of ventilation air. The first LAFSW configuration that was simulated using the LAMWIN program was essentially the last case discussed in Section 3.3.5.3. The window dimensions are 10 m-wide by 1-m high and the laminar air flow gap thickness is 9 mm. The thickness of the sealed air space between the inside and middle panes is 12.7 mm (1/2 in.) in this case and in all the other configurations that were simulated. As shown in Table 3.3, the U-value of this window is 1.25 $W/(m^2 * K)$ at the conditions simulated. The U-value is based on the heat flux from the outer pane to the surroundings in the absence of solar radiation. The supply air exit temperature without the presence of solar radiation is -10.4°C and with solar radiation is -5.7°C. These two cases are referred to as "NIGHT" and "DAY" respectively. Changing the window dimensions to 5 m wide by 2 m high has a negligible effect on these performance parameters. The laminar air flow in the higher 5- by 2-m window has a higher Reynolds

Table 3.3. Super Window Performance for Different Dimensions and Gap Widths and a Supply Air Flow Rate of 35 l/s

Gap Width [mm]			Window Dimensions Width by Height	
			10-m by 1-m	5-m by 2-m
9.0	Supply Air Exit Temperature [°C]	NIGHT	-10.4 (Gr/Re=7.36)	-10.4 (Gr/Re=3.68)
		DAY	-5.7 (Gr/Re=9.74)	-5.7 (Gr/Re=4.87)
	U-Value [W/(m^2*K)]		1.25	1.25
10.7	Supply Air Exit Temperature [°C]	NIGHT	-10.4 (Gr/Re=13.0)	-10.4 (Gr/Re=6.49)
		DAY	-5.8 (Gr/Re=17.2)	-5.8 (Gr/Re=8.58)
	U-Value [W/(m^2*K)]		1.21	1.21
13.5	Supply Air Exit Temperature [°C]	NIGHT	-10.5 (Gr/Re=27.6)	-10.5 (Gr/Re=13.8)
		DAY	-6.0 (Gr/Re=36.4)	-6.0 (Gr/Re=18.2)
	U-Value [W/(m^2*K)]		1.17	1.17

number based on the flow gap thickness, and therefore the supply air picks up less heat per unit height than in the shorter 10- by 1-m window, but the window has a greater height over which heat can be picked up from the middle pane and the overall performance is almost identical. The temperature profiles across the laminar air flow gap at different streamwise locations for the 10-m by 1-m window are shown in Figure 3.8 for the nighttime simulation and in Figure 3.9 for the daytime simulation. For a given gap thickness, the greatest increase in the supply air temperature per unit window height would be achieved by minimizing the Reynolds number. However, this would also tend to increase the U-value of the window, a performance parameter which is of secondary importance in the proposed application of the LAFSW as a ventilation air preheater, but one which must still be kept within a reasonable range to make the window economically practical. For a given gap thickness, the minimum allowable Reynolds number is governed by the hydrodynamic stability criterion for the flow.

Table 3.4 shows the window width required to provide a ventilation rate of 35 l/s for laminar air flow gaps ranging from 0.005 mm to 0.015 mm for a constant Grashof-to-Reynolds number ratio of 12. A safety margin was added to Tjelflaat and Bergesen's criterion that the ratio Gr/Re must be less than 24 to avoid hydrodynamic instability in full-developed channel flow between walls at differing temperatures, because the flow is developing in the present situation [4]. Subject to this condition, the practical lower limit on the laminar air flow gap thickness is approximately 11 mm, since at smaller thicknesses, the window width necessary to achieve the required ventilation rate at the minimum allowable Reynolds number becomes unreasonable.

The performances of four more window configurations having a total area of 10 m^2 and providing a total 35 l/s of ventilation air were investigated: two 10-m wide by 1-m high and the other two 5-m wide by 2-m high. For a nominal Gr/Re ratio of 12, the required laminar air flow gap thickness was calculated to be 10.7 mm for the 10-m by 1-m window and 13.5 mm for the 5-m by 2-m window. The effect of decreasing the laminar flow layer stability on the window performance by increasing

Table 3.4 Window Width Required to Provide a Ventilation Rate of 35 l/s for a Nominal Grashof-to-Reynolds Number Ratio of 12

LAMINAR AIR FLOW GAP, L [m]	NOMINAL GRASHOF NUMBER, Gr* [-]	REYNOLDS NUMBER, Re [-]	UNIFORM INLET VELOCITY, U [m/s]	VOLUMETRIC FLOWRATE PER m WINDOW WIDTH [m^2/s]	REQUIRED WIDTH FOR 0.035 m^3/s OF VENTILATION, W [m]
0.005	349	29.1	0.0710	0.355×10^3	98.6
0.007	956	79.1	0.139	0.973×10^3	36.0
0.009	2033	169	0.229	2.06×10^3	17.0
0.011	3711	309	0.343	3.77×10^3	9.28
0.013	6126	511	0.480	6.24×10^3	5.61
0.015	9411	784	0.638	9.57×10^3	3.66

* Nominal Grashof Number calculated assuming that the mean air temperature in the laminar air flow layer is 260 K and the mean temperature difference across the gap is 11 K.

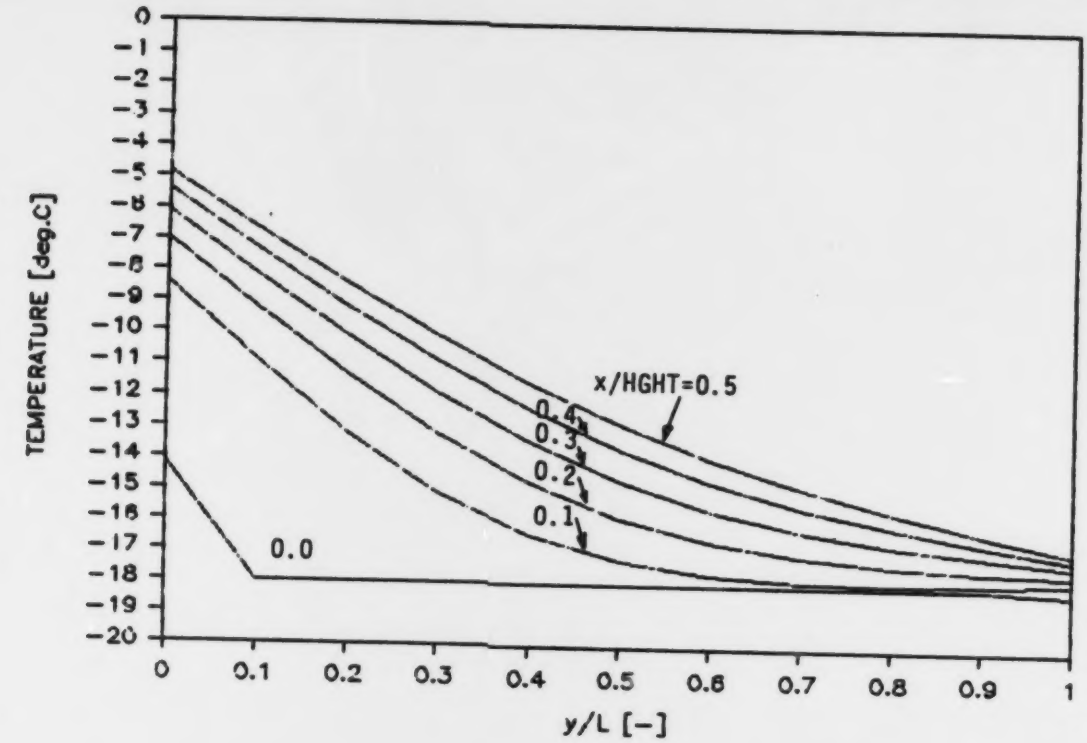

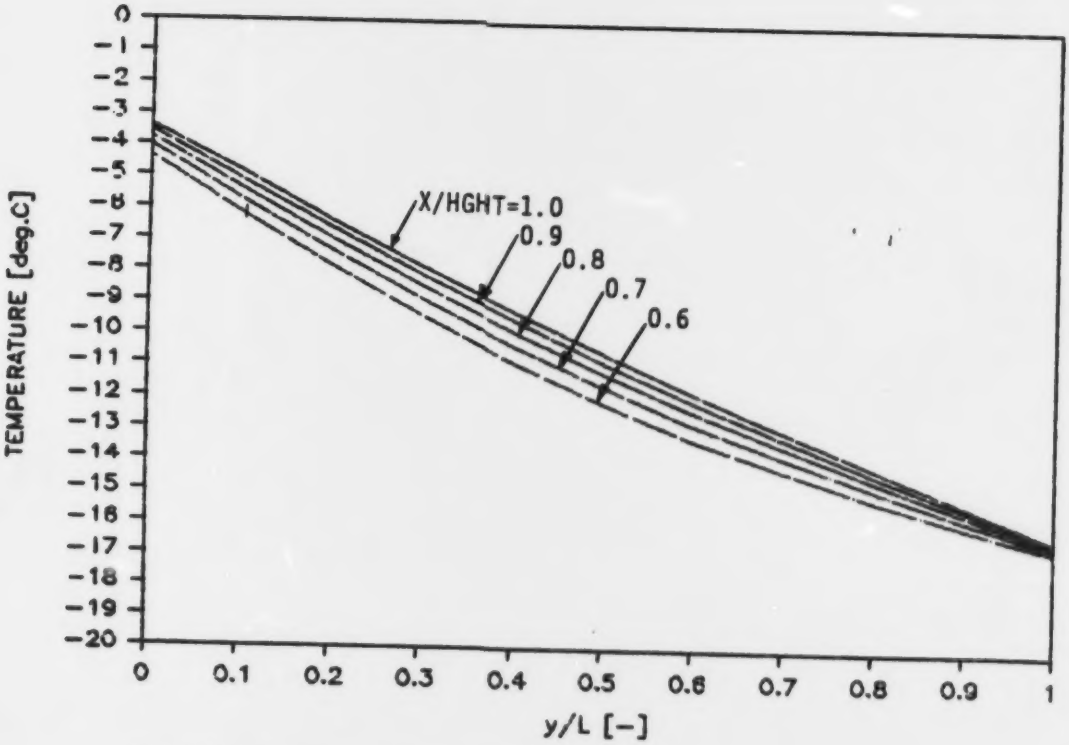

Figure 3.8 Temperature Profiles Across the Laminar Air Flow Gap for 1-m by 10-m Window with 9-mm Gap and Nighttime Simulation Conditions

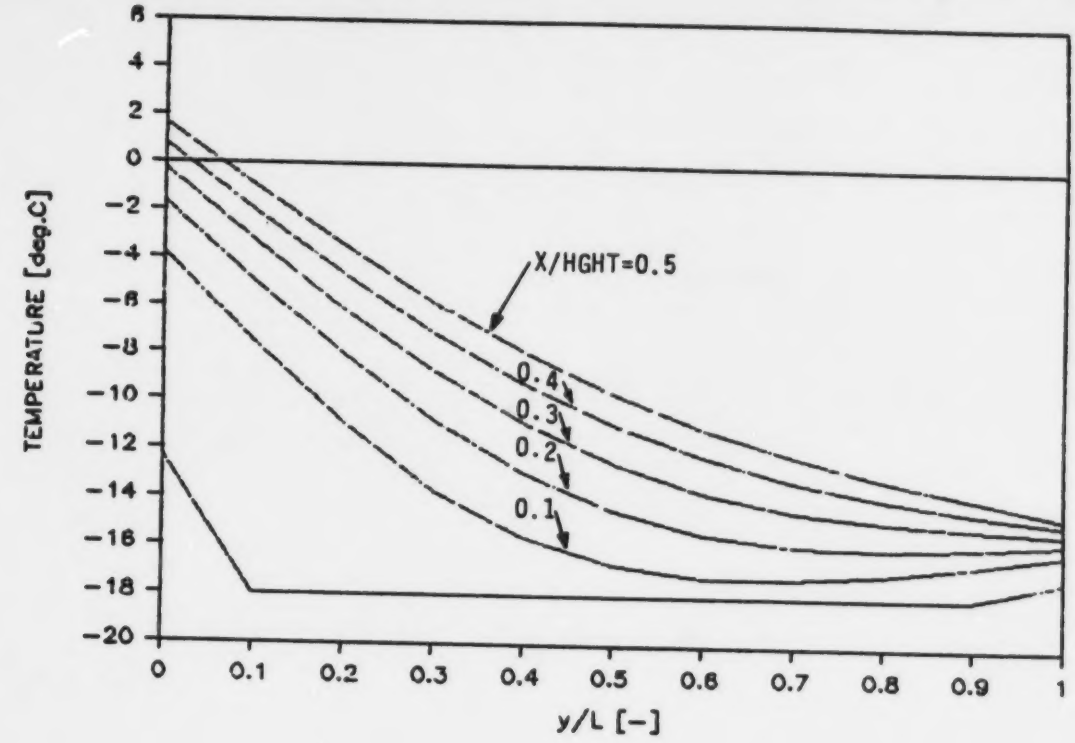

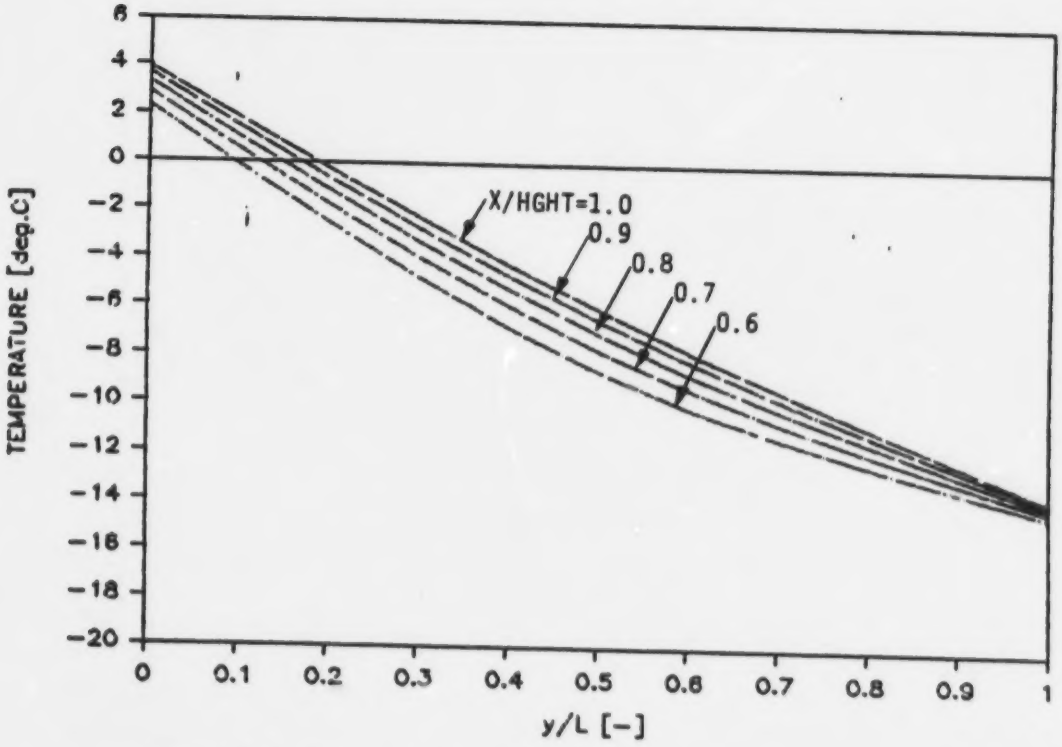

Figure 3.9 Temperature Profiles Across the Laminar Air Flow Gap for 1-m by 10-m Window with 9-mm Gap and Daytime Simulation Conditions

the nominal Gr/Re ratio to 24 was also investigated by simulating a 10-m by 1-m window with a 13.5-mm thick gap. Similarly, the effect of increasing the laminar flow layer stability on the window performance by decreasing the nominal Gr/Re ratio to 6 was investigated by simulating a 5-m by 2-m window with a 10.7-mm thick gap. The results are included in Table 3.3. The actual Gr/Re ratios based on the mean temperature of the middle and outside glazings are included under each of the supply air exit temperatures.

The results for the 10.7- and 13.5-mm laminar air flow gaps also indicate that for a given laminar air flow gap thickness, there is a negligible difference between the performance of a 10-m by 1-m window and a 5-m by 2-m window. As expected, the 13.5-mm gap width gives the window a lower U-value than the 9.0- or 10.7-mm gaps because the thermal boundary layer developing along the outer surface of the middle pane must grow to a greater thickness to reach the outside pane. This also results in the supply air exit temperature being slightly lower for the 13.5-mm gap. However, overall there is not a significant difference between the performance of the six configurations.

The thermal performance of the six previously-described LAFSW configurations was also resimulated with a low emittance coating on the outside surface of the middle pane. As in the simplified analysis of low E coated windows, this middle glazing was modeled as having a normal solar transmittance of 0.60, and normal reflectances of 0.25 and 0.22 with respect to solar radiation incident from the coating and substrate sides, respectively. The long-wave emittance of the low E coating was set at 0.35. All other window properties remained unchanged.

Table 3.5 summarizes the performances of the windows with a low E coating. As in the uncoated window simulations, there is negligible difference between the performance of a 10-m by 1-m window and a 5-m by 2-m window for a given gap width. The Gr/Re ratios based on the mean temperatures of the middle and outside glazings are included under each of the supply air exit temperatures. Considering Tjelflaat and Bergesen's criterion that the ratio Gr/Re must be less than 24 to avoid

Table 3.5 Super Window Performance for Different Dimensions and Gap Widths, a Supply Air Flow Rate of 35 l/s and a Low Emittance Coating on the Outside Surface of the Middle Pane

Gap Width [mm]			Window Dimensions Width by Height	
			10-m by 1-m	5-m by 2-m
9.0	Supply Air Exit Temperature [°C]	NIGHT	-9.4 (Gr/Re=8.87)	-9.4 (Gr/Re=4.43)
		DAY	0.97 (Gr/Re=16.2)	0.97 (Gr/Re=8.11)
	U-Value [W/(m^2*K)]		0.97	0.97
10.7	Supply Air Exit Temperature [°C]	NIGHT	-9.3 (Gr/Re=15.8)	-9.3 (Gr/Re=7.90)
		DAY	1.0 (Gr/Re=28.8)	1.0 (Gr/Re=14.4)
	U-Value [W/(m^2*K)]		0.91	0.91
13.5	Supply Air Exit Temperature [°C]	NIGHT	-9.3 (Gr/Re=34.0)	-9.3 (Gr/Re=17.0)
		DAY	0.81 (Gr/Re=61.7)	0.80 (Gr/Re=30.8)
	U-Value [W/(m^2*K)]		0.83	0.83

hydrodynamic instability in fully-developed channel flow between walls at differing temperatures, only the 9.0-mm gap is feasible for the practical implementation of a laminar air flow gap.

The total energy saving achieved by using a LAFSW without a low E coating in place of a conventional triple-glazed window can be evaluated by considering the reduced U-value of the glazing area and the energy gained by the preheated ventilation air. This energy saving can be expressed as follows:

$$U_{save} = (U_T - U_S) + P_L/(A\Delta T_{i-o})$$

where U_{save} is the energy saving rate per unit window area per degree indoor-to-outdoor temperature difference [$W/(m^2 * K)$],

U_T is the U-value of a conventional triple glazed window [$W/(m^2 * K)$],

U_S is the U-value of the LAFSW [$W/(m^2 * K)$] based on the heat flux through the innermost glazing,

P_L is the heat pickup rate of the supply air [W],

A is the window area [m^2],

and ΔT_{i-o} is the indoor-to-outdoor temperature difference [°C].

The energy saving rates, U_{save}, based on the previous simulations of LAFSWs with laminar air flow gaps of 9.0, 10.7 and 13.5 mm were calculated. The U-value of a conventional sealed triple-pane window was assumed to be 1.85 $W/(m^2 *K)$. In this table, the window dimensions have been removed as a variable, since they have an insignificant effect on the overall thermal performance of the window. Although the 13.5-mm gap provides the greatest energy saving rate, the 9.0-mm gap is recommended for the practical implementation of the laminar air flow layer because it is much more hydrodynamically stable than the other two thicknesses, and still provides a comparable energy saving rate.

Note that U_S, the U-value of the LAFSW, is calculated from the flux passing through the innermost glazing. This value is different from previously mentioned values of U, which were calculated from the flux passing through the outermost glazing.

Table 3.6 also includes the annual costs savings achieved by using a LAFSW in place of a conventional triple pane window. These cost savings, $C_{save(\$)}$, were calculated as follows:

$$C_{save} = (0.25U_{save,DAY} + 0.75U_{save,NIGHT})(A)(DD)(E_r)(24/1000)$$

where $U_{save,DAY}$ is the energy saving rate per unit window area per degree indoor-to-outdoor temperature difference for DAYtime conditions [$W/(m^2 * K)$],

$U_{save,NIGHT}$ is the energy saving rate per unit window area per degree indoor-to-outdoor temperature difference for NIGHTtime conditions [$W/(m^2 * K)$],

A is the window area (10 m^2),

DD is the heating degree days for the location under consideration (6000 °C-days for Winnipeg),

E_r is the electric energy cost (approximately .03/kWh in Winnipeg),

and the last term is a unit conversion.

The series present worth of the annual energy savings, also shown in Table 3.6, was calculated assuming a lifetime of 10 years for the window, a 4% inflation rate for domestic electric energy and a 10% interest rate. These numbers show that the LAFSW does not provide overwhelmingly high economic benefits. However, the LAFSW design could be economically feasible, depending very much on how its manufacturing cost would compare to that of a conventional triple-glazed sealed window, and how inexpensively the supply air ducting from the laminar air flow gap exit to the heat exchanger inlet could be installed.

Table 3.6. Cost Savings Achieved by Different Laminar Air Flow Gaps (based on electricity at $0.03/kWh)

GAP WIDTH [mm]	ANNUAL COST SAVING [$]	PRESENT WORTH OF SAVINGS OVER NEXT 10 YEARS [$]
9.0	72.15	537
10.7	73.87	550
13.5	74.95	558

4.0 DEVELOPMENT AND INSTALLATION OF PROTOTYPE WINDOW

4.1 The Prototype Window Design

The LAFSW provides a modest saving in energy. It must be manufacturable at low cost to return a reasonable payback. Therefore only the simplest of design configurations were considered. After several discussions with Mr. Bill Fast and Mr. Dan Friesen of Willmar Windows, the design of Figure 4.1 was selected. This design involves only 5 extra pieces of wood, with a total additional cross-sectional area of 0.0033 m^2 (5.1 in^2). This is a negligible increase in wood in a 1-m by 1-m window. Mr. Friesen has estimated that Willmar could manufacture these windows at an additional cost of $40.00 for a window of that size.

4.2 Installation of the Prototype

A window unit containing an openable window on one side and a 1.6-m high by 1.0-m wide LAFSW on the other side was manufactured by Willmar Windows and installed at 34 McMasters Road in November of 1986. This unit was left in place for a month without a fan system on it. During this time air flowed out through the window because it was above the neutral pressure plane of the house. This resulted in occasional frosting of the outer pane, and occasional icicles hanging from the air inlet on the outside of the house. After the fan and heater (see Figure 4.2) were installed, the air flow was in the proper direction and these problems disappeared. No negative effects of any kind were noticed, except that one of the residents felt that the ductwork, fan and heater were ugly. This is a problem that will easily be solved in future models.

A second problem was caused by inadequate sealing of the LAFSW at the bottom, so that air leaked in through a narrow slot instead of flowing in smoothly through the filter. Until it was sealed, this opening caused a disturbed air flow pattern between the panes, reducing the flow rate at which laminar flow could be maintained.

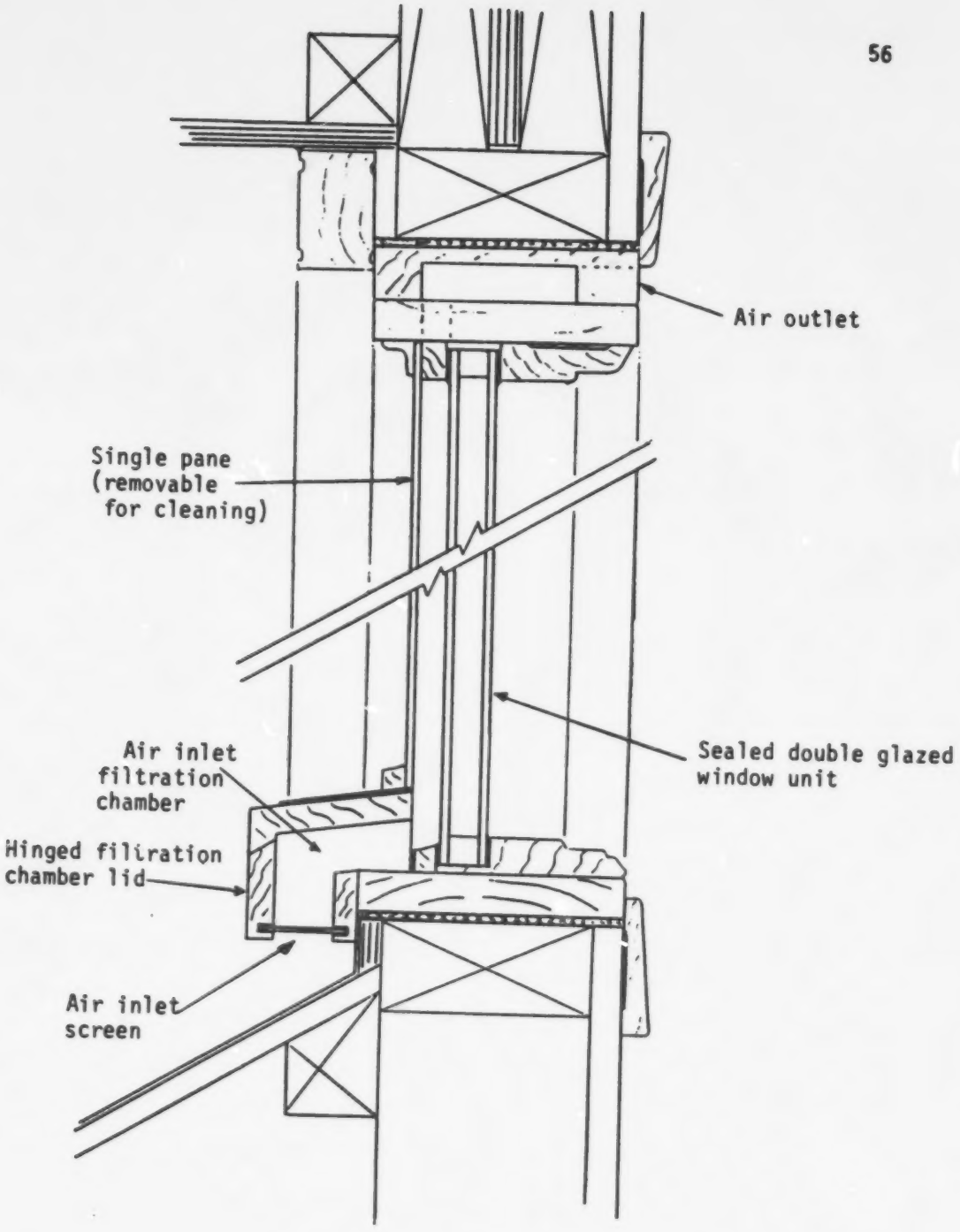

Figure 4.1 Vertical cross-sectional view of prototype laminar air flow window. The window ducting is not shown in this view.

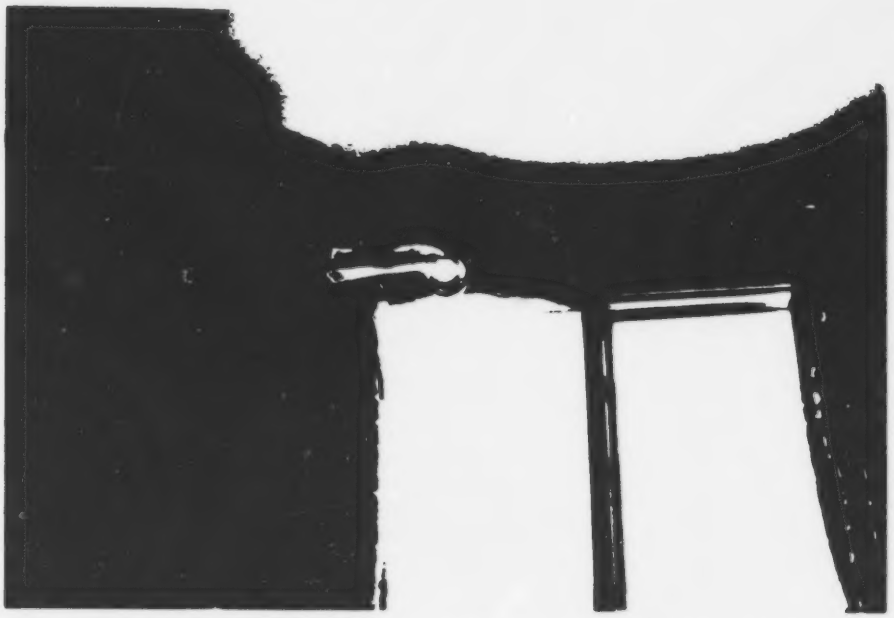

Figure 4.2a Interior View Showing Ducting, Fan and Heater

Figure 4.2b Exterior View LAFSW on Right

Figure 4.2 The LAFSW in Place

5.0 VENTILATION SYSTEM

5.1 Initial Review

Three possibilities were considered initially for distributing the air admitted by the ventilator window. One was to install a fan and heater with each window and eject the air directly into the room. The second was to duct the air from each LAFSW to a central heat recovery ventilator (HRV). The third was to duct the air from each LAFSW to the furnace air distribution system.

All three approaches were based on the assumption that the air entering through the LAFSW would be too cold to dump directly into the room. Since the LAFSW heats the air as little as 8°C, it could be very cold on the coldest days of winter. This assumption was made without testing and, as it turned out later, may not be true.

Each of these approaches presents several difficulties. The use of a local fan and heater is expensive. We have estimated the overall cost of the assembly at about $50.00. This is greater than the incremental cost of the LAFSW itself and would prevent the system from being cost effective on any but the largest windows.

This approach can be applied in a retrofit condition, but some people may consider the use of plug-in electrical wiring unsightly. If so, wire would have to be fished through the wall and installed behind baseboards. This would also be expensive.

The second approach, feeding the incoming air to an HRV, could only be applied economically in new-house construction; and the cost of ducting could only be justified for very large windows. One benefit of this system would be that it would reduce the heat exchanger frosting problem. In some locations it might even eliminate it completely, so that the HRV could be manufactured without a defrost mechanism.

The saving that would result from eliminating the HRV defrost mechanism would probably pay for the LAFSW and ducting required to achieve it. However, it would require a substantial simulation effort, beyond the scope of this project, to determine in which climates this would be possible.

In a new house, it would cost about $120 per window connected to vent the windows to the HRV. This would reduce the economic benefits from the LAFSW to zero on a window of $2.2m^2$, and substantially reduce the benefits on larger windows.

Feeding the air to the furnace ducting has the same disadvantages as feeding it to an HRV. Furthermore, the saving due to eliminating defrost is not available in this case. Also, the furnace fan would have to run continuously at the same speed if this approach were used. Many people object to the drafts which this mode of operation creates.

A review of these three options is discouraging. It leads to the conclusion that the main obstacle to the introduction of the LAFSW is the cost of introducing the incoming air into the house.

5.2 Humidity Controlled Air Inlets

After the initial review of the ventilation options had been carried out, a new ventilation system was located which appears to eliminate these difficulties. This system is based on humidity-controlled air inlets (HCAI). When this system is used, the pressure in the house is maintained at a negative value by an exhaust fan. Two kinds of exhaust fans are used. One uses a constant volume controller that maintains a constant flow regardless of house pressure changes. The second uses a humidistat in the exhaust air duct to control the air flow.

An HCAI is installed in each room. These inlets have no fans. Flow is induced through them by the negative pressure produced by the exhaust fan. The air inlets in unoccupied rooms sense the reduction in

humidity in these rooms and reduce the air supply accordingly. In occupied rooms, the moisture production results in increased humidity which, in turn, causes the air inlets to open wide.

This system has the potential to provide improved indoor air quality with reduced ventilation. The fresh air is directed to the occupied rooms, so that the people in the house experience a high air change rate while the house as a whole has a low one.

This advantage would be lost in a house with a forced-air furnace, since the air recirculation system would quickly mix the air throughout the house. However, the HCAI system of ventilation also eliminates the major disadvantage of electric baseboard heating compared to a forced-air furnace, which is the reduced air circulation and resulting lower local air quality. Thus, local humidity-controlled ventilation with baseboard heat can save energy by allowing local control of both ventilation and temperature.

Two systems which operate as described above are presented in Appendix A.

At first glance it might seem that this system would create cold drafts in the rooms to which the inlet air is admitted, since the humidity-controlled air inlets have no heating devices. However, the manufacturers claim that this is not the case. The cold air is directed diagonally at the ceiling so that it spreads across the ceiling, mixing with the warm room air before it contacts the occupants. The flow rate would be of the same magnitude as the infiltration flow into a pre-1975 house ventilated by infiltration. In fact it would be less in the colder months, since most houses are overventilated and become dry in midwinter, whereas the system described above would still provide just the right amount of air for moisture removal.

We have not seen these systems applied in the colder Canadian climates. There is a dealer who installs them in Vancouver, and the American dealer claims many successful installations in the northern

United States, but it is yet to be proven that the system will not create unpleasant drafts in severe cold weather.

In an attempt to obtain a preliminary assessment of the seriousness of this problem, the LAFSW which was installed as part of the present problem was operated for several weeks with the heater removed and the air outlet directed at the ceiling. The lowest ambient temperature experienced during this test was -25°C.

No significant discomfort was noted during this period. It was noted that the bedroom with the LAFSW dropped slightly in temperature compared to the rest of the house, but this effect would be eliminated by the use of a baseboard heater with a local thermostat, instead of a furnace with a central thermostat. It was also found that there was a slight downdraft of cold air below the outlet. This was cuased by the phenomenon known as "dumping," in which cold ventilation air which is moving too slowly will fall from the ceiling due to its higher density. In the present case, this effect was caused by using a 75 mm duct directed straight up as an air outlet. A slot nozzle which directed the air along the ceiling would eliminate this problem.

Neither of these problems was serious enough to be noticed by the occupants. They were found only by a search with a thermometer and a smoke pencil. From this preliminary trial, it appears likely that the LAFSW/HCAI combination can be used without discomfort.

The advantages of combining the HCAI system with the LAFSW are obvious. The LAFSW now needs no additional equipment to distribute the air. The HCAI is simply installed on the outlet of the LAFSW. The heat addition in the LAFSW will extend the range of temperatures over which the humidity controlled ventilation system can be used.

5.3 Cost Analysis

The basis for our cost analysis is that the humidity controlled ventilator system is itself cost effective. The primary evidence for

this is the fact that 60,000 of them have been installed since they were introduced onto the market in 1983.

The price of the humidity controlled air inlets is $39.00 U.S. (retail) and the price of a typical exhaust fan system with four sets of ducting is $500 U.S. installed. The cost of this system is partly offset by the reduced cost of a baseboard heating system relative to that of a central forced air system. (This difference is about $450.00 in Manitoba.) The remainder of the price is justified by the improvement in air quality and the reduction in the ventilation air requirement and the cost of heating it.

Based on the assumption that this ventilation system justifies its own cost, the analysis of the economics of the LAFSW becomes very simple. The only additional cost is the extra cost of the windows themselves, which is about $40.00 per m^2.

The present value of the savings has been conservatively estimated at $53.70 per m^2, so this indicates that the economic benefits of the LAFSW are reasonable. This estimate was based on the Manitoba electricity cost of $0.03 per kWh, which is the lowest in Canada. Elsewhere the economic benefits will be greater.

6.0 DISCUSSIONS WITH MANUFACTURERS

It was originally planned that the last part of this project would be to recruit a manufacturer to participate in the second phase. However, this has proved to be impossible due to a simple obstacle. The manufacturers want to see the report of this study before they seriously consider getting involved. We have had discussions with three manufacturers (Willmar, Loewen and Dorwin) and all are interested, but none are prepared to make a commitment until they have had a chance to review the results of this project.

On the other hand, the American Aldes Corporation, which markets a humidity-controlled ventilation system, has made a commitment in principle to be involved in the development and testing of the system we propose. The same is true of Flair Homes, an innovative Winnipeg house builder, who are prepared to build a house to test the system.

In spite of the present caution of the window manufacturers, we have no doubt that we will find one who wishes to take part in the second phase of this project.

7.0 INTERPRETATION OF THE PROJECT RESULTS

7.1 Theoretical and Practical Feasibility of the Window Concept

This concept has been tested for practical feasibility by constructing a LAFSW and installing and testing it in a house. After one winter of operation, no practical difficulties have been encountered, so it appears that the concept is practically feasible.

There are several limits on the design of the LAFSW. One is that the Reynolds Number must be well below 2000. This puts an upper limit on the volume flow rate per unit width of window. A second limit is that the ratio of the Grashof Number to the Reynolds Number must be less than 24, to avoid flow instability. Since the Grashof Number is proportional to the plate spacing cubed, this puts an upper limit on the plate spacing. Since it also prevents the Reynolds Number from being reduced too much, it puts a lower limit on the volume flow rate per unit width.

To conform with normal house design practices, the height, width and total area of windows are also restrained. A final restraint is that a house has a specific requirement for ventilation air.

It is fortuitous that in spite of all these restrictions, a high efficiency LAFSW is feasible. It turns out that the ventilation flow rates and window sizes for typical houses combine to produce Reynolds Numbers in the laminar range. Furthermore, a plate spacing in the range of 10 mm, which is consistent with present practice, keeps the ratio of Grashof Number to Reynolds Number in the stable range.

The heat transfer analysis which was carried out in this project has shown that, within the dimensional and fluid flow limits described above, it is possible to achieve net heat losses far lower than those achieved with conventional triple glazed window. Thus the concept can be considered to be theoretically feasible.

7.2 Economic Feasibility

A major barrier to creating an economically feasible LAFSW system was the fact that LAFSWs provide a small amount of ventilation air to each room. The cost of collecting this air and delivering it to a central point prevented the system from being economic.

When the "humidity-controlled supply air" approach was considered, what had previously been a problem became an asset. In this system, fresh air inlets are required in all rooms, so that each LAFSW will be equipped with its own humidity-controlled inlet.

The economic analysis therefore considered only the cost of the LAFSW itself. Based on this approach, and using a conservative estimate of the present value of the reduction in the cost of energy, the LAFSW is definitely economically feasible.

7.3 Continuation to Second Phase of LAFSW Evaluation

In the original proposal for the LAFSW project, a second phase was described. In this proposed second phase, a window manufacturer was to make an LAFSW and its thermal performance was to be measured. This thermal performance was to be compared with that predicted by the simulation program used in Phase 1.

It is now apparent that there is another important element to Phase 2. This is the testing of the combined LAFSW/humidity-controlled ventilation system in a whole house. This testing will be aimed primarily at verifying that the system can deliver fresh air to the house without creating discomfort even in very cold weather, and that it can maintain equivalent indoor air quality at a lower net cost than a conventional HRV system.

Since the results of this test will only apply specifically to the house tested, part of this project will be the development of a pollutant concentration computer model which will be verified against

the results obtained and can be used to extend the results to other house designs. This computer model will predict the flow rates required through the LAFSW to maintain satisfactory indoor air quality in any house.

It was planned that the last part of Phase I of this project would be the recruiting of a manufacturer to take part in Phase II. However, although several manufacturers were very interested in the project, none was willing to make a financial commitment until he had seen the Phase I report. Therefore, the recruitment of a manufacturer to participate in Phase II, and the detailed planning of the Phase II project, will take place after the present report has been submitted.

8.0 CONCLUSIONS

The conclusions to be drawn from the work carried out in this project as are follows:

a) It is possible to build and operate a LAFSW within the practical limits of window dimensions and house ventilation requirements.

b) Window heat loss can be reduced very substantially by installing LAFSWs.

c) The cost of manufacturing LAFSWs is low enough to make their use cost effective.

d) By combining the LAFSW with local ventilation using humidity-controlled air inlets, the incoming fresh air can be used without a prohibitively expensive system of ducting.

9.0 RECOMMENDATIONS

Considering the four conclusions listed above, it is recommended that the LAFSW project continue to the second phase, and that this second phase include the laboratory testing of the thermal performance of an LAFSW and the testing of an LAFSW ventilation system in a house.

REFERENCES

1. R. Johnson, "Multiple Glazing Systems with Between Panes Ventilation", Lawrence Berkeley Laboratory, LBID-166 EEB-W-80-09 W-61, November 1979.

2. J. F. Peck, T. L. Thompson, H. J. Kessler, "Windows for Accepting or Rejecting Solar Heat Gain: Final Report", Lawrence Berkeley Laboratory, LBL-15440 UC-95d, September 1982.

3. J. Gabrielsson, "Extract Air Window, A Key to Better Heat Economy in Buildings", 10th World Energy Conference, Istanbul, Sept. 19-23, 1977.

4. R. F. Boehm, K. Brandle, "Testing of Air Flow Windows for Evaluation and Application", Lawrence Berkeley Laboratory, LBL-12065.

5. O. Seppanen, "Windows as Cost Effective Solar Collectors", Proceedings of the Sixth National Passive Solar Conference, American Section of the Int. Sol. Energy Soc.

6. W. F. Chapman, "Less Refrigeration: More Glass, A Compatible Idea?", ASHRAE Journal, Feb. 1979.

7. D. Sodergren, T. Bostrom, "Ventilating with the 'Exhaust Air Window'", ASHRAE Journal, Apr. 1971.

8. P. O. Tjelflaat, B. Bergesen, "Improved Thermal Insulation in Windows by Laminar Air Flows", Thermal Performance of the Exterior Envelopes of Buildings III, Clearwater Beach, Florida, Dec. 1985.

9. "VISION: A Computer Program to Evaluate the Thermal Performance of Super Windows", final report prepared by Spider Engineering Associates (Waterloo) Inc. for SEP, NRC, Aug. 1983.

10. J. L. Wright, "Effective U-Values and Shading Coefficients of Preheat/Supply Air Glazing Systems", Proceedings of the Renewable Energy Conference, Winnipeg, Man., 1986.

11. G. S. Beavers, E. M. Sparrow, R. A. Magnuson,"Experiments on the Breakdown of Laminar Flow in a Parallel Plate Channel", Int. Journ. Heat Mass Transfer, Vol. 13, pp 809-815. Pergamon Press 1970.

12. L. B. Gdalevich, E. F. Nogotov, V. E. Fertman, "Effect of Side Walls on Heat Transfer Through a Vertical Air Layer in Laminar Natural Convection", Int. Journ. Heat Mass Transfer, Vol. 22, pp. 1601-1606, Pergamon Press 1979.

13. J. Sucec, A. M. Sawant, "Unsteady, Conjugated, Forced Convection Heat Transfer in a Parallel Plate Duct", Int. Journ. Heat Mass Transfer, Vol. 27, No. 1, pp. 95-101, 1984.

14. K. H. Im, R. K. Ahluwalia, "Combined Convection and Radiation in Rectangular Ducts", Int. Journ. Heat Mass Transfer, Vol. 27, No. 2, pp. 221-231, 1984.

15. M. N. Ozisik, Ch. Trepp, H. Egolf, "Laminar Forced Convection in Converging or Diverging Planar Symmetric Ducts", Int. Journal Heat Mass Transfer, Vol. 25, No. 10, pp. 1477-1480, 1982.

16. J. R. Sellars, M. Tribus, J. S. Klein, "Heat Transfer to Laminar Flow in a Round Tube or Flat Conduit-The Graetz Problem Extended", Trans. Am. Soc. Mech. Engrs. 78, pp 441-448, 1956.

17. W. E. Mercer, W. M. Pearce, J. E. Hitchcock, "Laminar Forced Convection in the Entrance Region Between Parallel Flat Plates", Journ. Heat Transfer, August 1967, pp 251-256.

18. M. S. Bhatti, C. W. Savery, "Heat Transfer in the Entrance Region of A Straight Channel: Laminar Flow With Uniform Wall Heat Flux", Transactions of the ASME, Feb. 1977, pp. 142-144.

19. M. S. Bhatti, C. W. Savery, "Heat Transfer in the Entrance Region of A Straight Channel: Laminar Flow With Uniform Wall Temperature", Journal of Heat Transfer, Vol. 100, pp 539-542, August 1978.

20. C. H. Liu, E. M. Sparrow, "Convective-Radiative Interaction in a Parallel Plate Channel-Application to Air-Operated Solar Collectors", Int. Journ. Heat Mass Transfer, Vol. 23, pp. 1137-1146, 1980.

21. A. P. Hatton, J. S. Turton, "Heat Transfer in the Thermal Entry Length with Laminar Flow Between Parallel Walls at Unequal Temperatures", Journal Heat Mass Transfer, Vol. 5, pp 673-679, Pergamon Press 1962.

22. P. O. Tjelflaat, B. Bergesen, "Improved Thermal Insulation in Windows by Laminar Air Flows", Thermal Performance of the Exterior Envelopes of Buildings III, Clearwater Beach, Florida, Dec. 1985.

23. D. K. Edwards. "Solar absorption by each element in an absorber-coverglass array", Technical Note, Solar Energy, Vol. 19, pp. 401 - 402.

24. E.M. Sparrow, S.H. Lin, and T. S. Lundgren, "Flow Development in the Hydrodynamic Entrance Region of Tubes and Ducts", The Physics of Fluids, Vol. 7, No. 3, March 1964, pp. 338 - 347.

25. J.R. Bodoia and J. F. Osterle, Appl. Sci. Res., Vol. 10, Sec. 1, 1961, pp. 265 - 276.

26. H. Morihara, and R. T.S. Cheng, "Numerical Solution of the Viscous Flow In the Entrance Region of Parallel Plates", Journal of Computational Physics, Vol. 11, 1973, pp. 550 - 572.

27. Y. L. Wang and P. A. Longwell, "Laminar Flow in the Inlet Section of Parallel Plates", A.I. Ch. E. Journal, Vol. 10, No. 3, May 1964, pp. 323 - 329.

28. A. Brandt and J. Gillis, "Magnetohydrodynamic Flow in the Inlet Region of a Straight Channel", The Physics of Fluids, Vol. 9, No. 4, April 1966, pp. 690 - 699.

29. ASHRAE Handbook, 1985 Fundamentals, American Society of Heating, Refrigeration and Air-Conditioning Engineers, Inc., 1985.

APPENDIX A

AERECO

175.4

Humidity-controlled air extractor

PATENTED

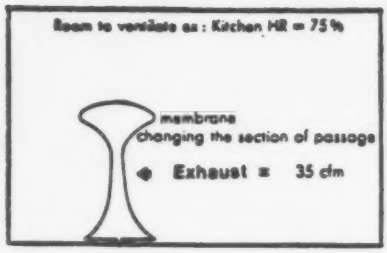

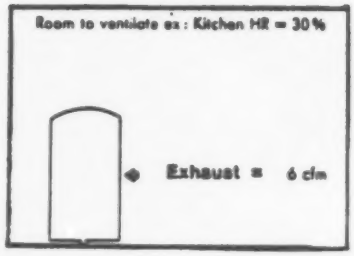

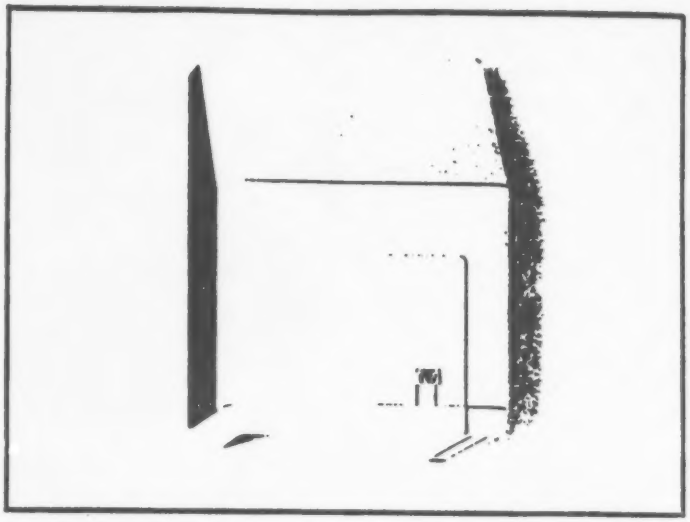

Humidity-controlled air inlet

PATENTED

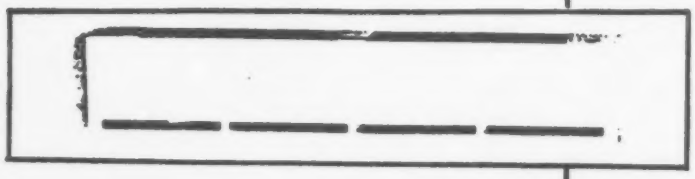

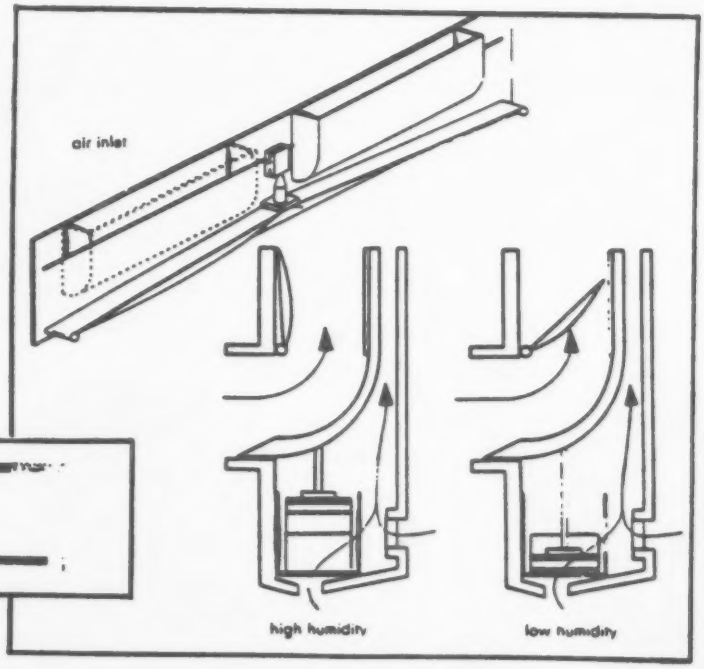

ENEREADY

ENEREADY PRODUCTS LTD • 5882 BRYANT STREET • BURNABY BRITISH COLUMBIA CANADA • V5H 1X6 • (604) 433-5887

The AERECO System is a self-regulating, humidity-controlled residential ventilation system. It is designed for use in wet, moderate climates where outdoor temperatures seldom drop below -20°C. (-4°F.)

AERECO monitors humidity in each room of the house and varies the room by room ventilation depending on the number of people, their activities and the outdoor weather conditions.

This system works well with all types of heating systems. The capital cost is approximately one-half that of a heat recovery ventilator and operating costs are approximately equal to those of a good quality HRV.

The AERECO System is made up of three major components:

1) FAN

A continuously operating fan located in the attic, utility room or crawlspace exhausts air from the moist rooms of the home (kitchen, bathrooms and laundry). Small ductwork links this fan to air extractors that moderate the exhaust air from these rooms.

2) AIR EXTRACTOR ●

An air extractor is installed in each moist room in a high-wall or ceiling location. The air extractor contains a humidity sensor which automatically varies the exhaust cfm; it all but closes when the room is dry and opens wide during cooking or showering. The ideal kitchen location is over the range, in combination with a recirculating hood fan. The kitchen air extractor varies from 6 - 35 cfm depending on humidity levels, with a manual over-ride to 80 cfm. The best bathroom location is directly over the bathtub or shower. The bathroom air extractor varies from 3 - 18 cfm depending on humidity levels, with a manual over-ride to 80 cfm.

3) AIR INLET ⇥

An air inlet is installed on an exterior wall in each of the living area rooms (living room, dining room, family room, bedrooms). Fresh air enters through a screened rain hood, passes through a sleeve in the exterior wall and enters the home via the controlled inlet. These inlets are NOT connected to a fan, but self-adjust by humidity, admitting air only to occupied rooms.

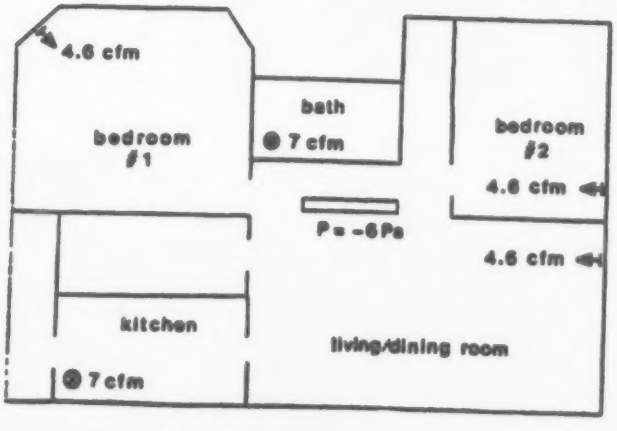

Example: DAY TIME

No one in the dwelling
Outside Temperature: 32°F.
Inside Temperature: 70°F.

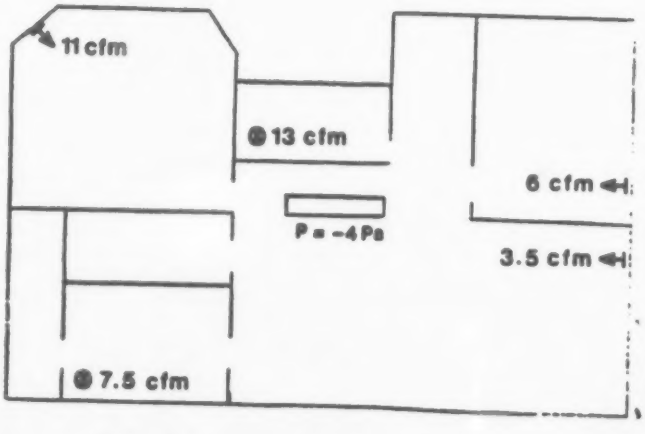

Example: NIGHT TIME

2 adults sleeping in bedroom #1
1 child sleeping in bedroom #2
Wet towels hanging in bathroom
Outside Temperature: 32°F.

EH

ENTRÉES D'AIR POUR SYSTÈME HYGRORÉGLABLE

DESCRIPTION PRODUIT

PRINCIPE

Un système de ventilation mécanique hygroréglable est un système simple flux où l'air neuf est admis dans les chambres et séjour par des entrées d'air hygroréglables, et l'air vicié extrait en cuisine et bains par des bouches d'extraction hygroréglables, en WC par une bouche minutée.

Ce système fait l'objet d'une autorisation ministérielle (du 29 mars 1984) précisant les types de matériels à mettre en œuvre ainsi que les débits à prendre en compte pour le calcul du coefficient G.

L'entrée d'air hygroréglable est l'élément d'un système de ventilation hygroréglable permettant la répartition de l'air suivant le taux d'humidité de chaque pièce principale (chambres et séjour).

En logement neuf ce type d'entrées d'air ne peut être utilisé que dans le cadre d'un système complet de ventilation hygroréglable, c'est-à-dire comprenant :
- un ventilateur spécial hygro,
- un réseau de conduits simple flux dimensionné «hygro»,
- des bouches d'extraction hygroréglables,
- des entrées d'air hygroréglables.

INTÉRÊTS

Un système complet de ventilation hygroréglable permet :

- **élimination des condensations**
  Les bouches d'extraction et les entrées d'air étant directement asservies au taux d'humidité de chaque pièce, la ventilation hygroréglable va permettre un contrôle continu et automatique des risques de condensation.
- **économie d'énergie**
  En s'adaptant parfaitement aux besoins, la ventilation hygroréglable ventile lorsque c'est nécessaire, là où c'est nécessaire. Elle permet d'éviter ainsi tout gaspillage d'énergie par excès de ventilation.
- **facilité d'installation**
  La ventilation hygroréglable est aussi simple à installer qu'une ventilation mécanique simple extraction.
- **facilité d'utilisation**
  La régulation des débits en fonction de l'hygrométrie s'effectue automatiquement.

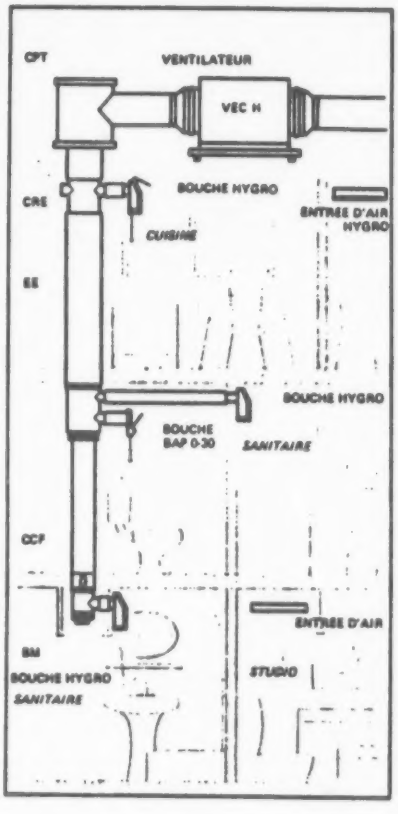

ENTRÉES D'AIR TYPE 5 - 30

DESCRIPTION

Les entrées d'air hygroréglables EH permettent de faire varier leur passage d'air de 5 cm² à 30 cm² suivant le taux d'humidité de la pièce où elles se trouvent.

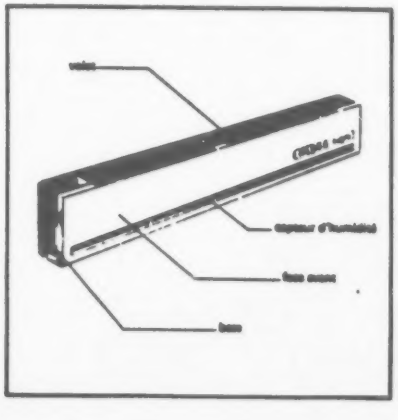

L'entrée d'air EH est composée de :
- une face avant en plastique de couleur beige,
- une base en plastique de couleur marron,
- un joint placé sur la face arrière de la base,
- deux volets permettant de faire varier la surface de passage d'air,
- un capteur d'humidité composé d'une tresse tendue sur un support en inox.

Son poids est de 250 grammes.

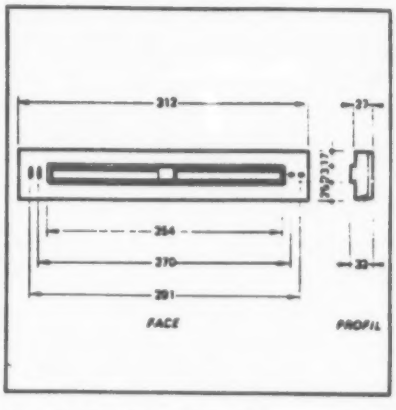

CARACTÉRISTIQUES

Entrée d'air «plaine» EHP

L'entrée d'air EHP est destinée à équiper tous les logements «hygro» se situant à une altitude inférieure à 1000 m.
Le réglage de la bouche a été effectué de telle sorte que l'entrée d'air offre un passage d'air de :

5 cm² pour 40 % d'humidité
30 cm² pour 75 % d'humidité

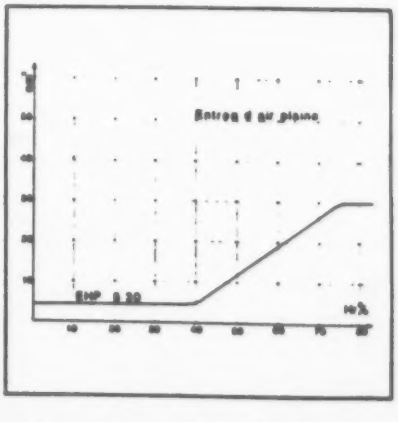

La forme du passage d'air a été conçue afin que l'entrée d'air puisse être soumise à une forte dépression sans risque de relief sonore (voir tableau n° 1).

Entrée d'air «montagne» EHM

L'entrée d'air EHM est destinée à équiper tous les logements «hygro» se situant à une altitude supérieure à 1000 m.
Le réglage de la bouche a été effectué de telle sorte que l'entrée d'air offre un passage d'air de :

5 cm² pour 25 % d'humidité
30 cm² pour 60 % d'humidité

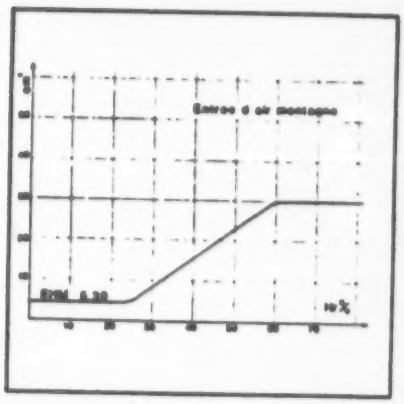

Le relief sonore de l'EHM est donné par le tableau n° 1 ci-dessous.

Surface	Humidité EHP	Humidité EHM	Relief sonore à 10 Pa dB(A)	Relief sonore à 20 Pa dB(A)	Relief sonore à > 40 Pa dB(A)
5 cm²	40 %	25 %	24	24	26
10 cm²	48 %	33 %	24	24	26
20 cm²	62 %	47 %	24	24	26
30 cm²	75 %	60 %	24	28	32

TABLEAU N° 1

Les mesures acoustiques sont faites dans un local de 25 m³ ayant une durée de réverbération de 0,5 s, le micro étant placé à 2,50 m.

CODE	DÉSIGNATION
14102	EHP 5-30
14103	EHM 5-30

ENTREES D'AIR TYPE STUDIO

Le studio ne possédant qu'une seule pièce principale, le rôle des entrées d'air dans un système hygro studio se limite à offrir une surface de passage d'air de 30 cm² sans risque de relief sonore pour de fortes dépressions.

ENTRÉE D'AIR STUDIO FAÇADE

L'entrée d'air studio type façade possède le même aspect et les mêmes côtes que les EH 5-30 cm².
Son relief sonore est identique à une EH 5-30 cm² lorsque celle-ci offre une surface de passage d'air de 30 cm².

NOTA : la mise en œuvre de l'entrée d'air studio est identique à celle des EH 5-30 cm².

ENTRÉE D'AIR STUDIO MENUISERIE

Elle se compose d'un déflecteur (sans régulateur) type 30 VM et d'un auvent type 30 VM en matière plastique de couleur blanche.

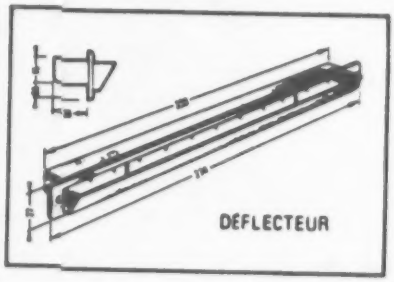

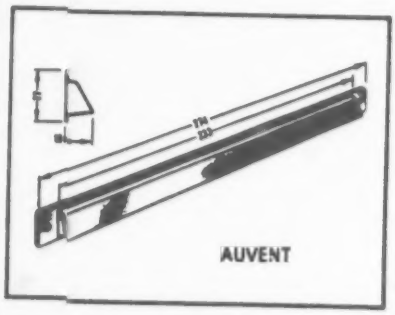

CODE	DÉSIGNATION
14101	EH studio façade
14104	Kit EH studio Menuiserie (auvent + déflecteur)

MISE EN ŒUVRE

La mise en œuvre des entrées d'air type EHM et EHP nécessite un certain nombre de précautions dues à la présence des capteurs d'humidité.
Pour être efficace, la ventilation hygroréglable impose une lecture exacte de l'humidité des différentes pièces principales, or l'humidité de l'air n'est pas répartie dans une pièce de façon homogène.
Toute mise en œuvre derrière un voilage sera à éviter.
L'installation au-dessus d'un convecteur ou tout autre appareil dégageant une forte chaleur est interdite.

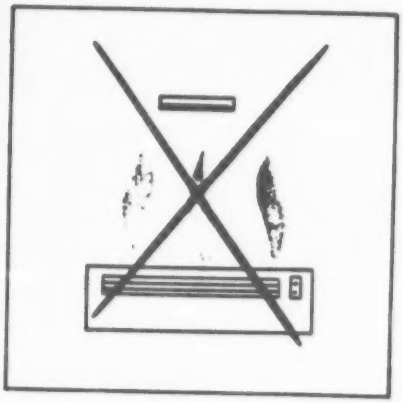

Ces cas étant repoussés, les mises en œuvre possibles sont :

- coffre de volet roulant,
- traversée de mur,
- haut de fenêtre,
- comble (pour les pavillons).

La fixation de l'entrée d'air se fait par 2 vis. Décliper la face avant pour introduire la vis dans les pré-défonçages se trouvant sur la base de l'entrée d'air hygroréglable.

COFFRE DE VOLET ROULANT

La face avant est fixée à la base par simple clipage.
Réservation : 255 x 24

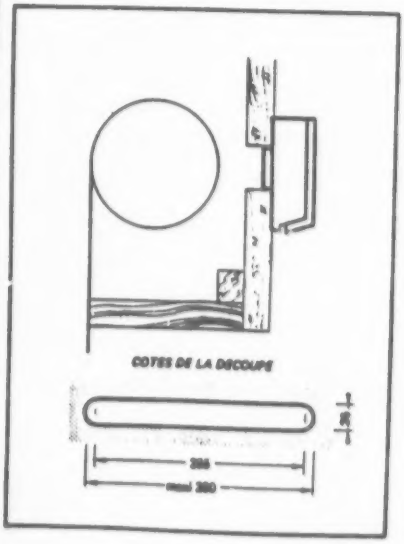

TRAVERSEE DE MUR

Manchon non acoustique

- manchon coulissant,
- corps en tôle galvanisée,
- auvent en matière plastique beige.

L'auvent et l'entrée d'air peuvent se fixer aussi bien sur la partie femelle que sur la partie mâle (isolation intérieure ou extérieure).

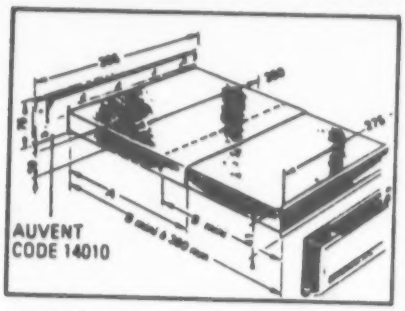

REMARQUES :

- Veiller à ne pas provoquer la déformation de la partie femelle lors de la mise en œuvre (placer une cale à l'intérieur).
- Lors de la mise en place, donner au manchon une légère pente vers l'extérieur.
- Il est conseillé d'assurer l'étanchéité entre l'auvent extérieur et la paroi par un mastic qui sera compressé lors du vissage de l'auvent.

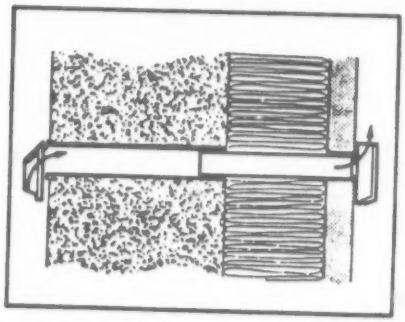

Réservation : 35 x 290 mm

CODE	TYPE	A cm	B mini cm	B maxi cm
14013	Manchon coulissant HYGRO	14	22	34
14014	Manchon coulissant HYGRO	15	22	35
14001	Manchon coulissant HYGRO*	16	22	36
14015	Manchon coulissant HYGRO	17	21	36
14016	Manchon coulissant HYGRO	18	20	36
14002	Manchon coulissant HYGRO*	19	19	36

*Disponible sur stock.

Manchon acoustique 39 dB (A)

- manchon coulissant,
- corps en tôle galvanisée,
- traitement acoustique : laine de verre,
- auvent en matière plastique beige.

L'auvent et l'entrée d'air peuvent se fixer aussi bien sur la partie femelle que sur la partie mâle (isolation intérieure ou extérieure)

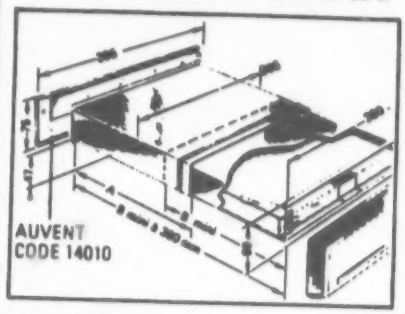

REMARQUES :

- Veiller à ne pas provoquer de déformation de la partie femelle lors de sa mise en œuvre.
- Veiller à ne pas détériorer la laine de verre située dans la partie mâle du manchon.
- Lors de sa mise en place, donner au manchon une légère pente vers l'extérieur.
- Il est prudent d'assurer l'étanchéité entre l'auvent extérieur et la paroi par un mastic qui sera compressé lors du vissage de l'auvent.

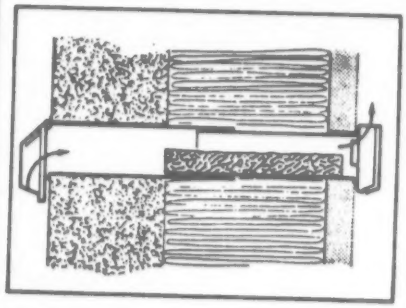

Réservation : 55 x 290 mm

Isolement acoustique obtenu Dn (route) : 39 dB(A).

Analyse par bande de fréquence : voir graphique ci-dessous.

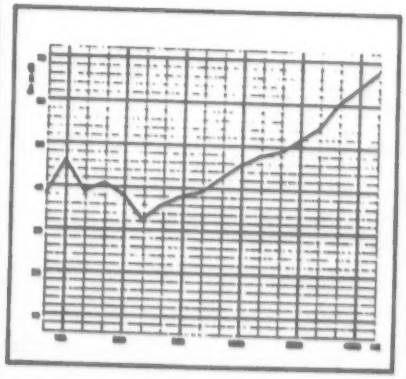

CODE	TYPE	A cm	B mini cm	B maxi cm
14017	Manchon coulissant acoustique HYGRO	14	24	36
14018	Manchon coulissant acoustique HYGRO	15	23	36
14003	Manchon coulissant acoustique HYGRO	16	22	36
14019	Manchon coulissant acoustique HYGRO	17	21	36
14020	Manchon coulissant acoustique HYGRO	18	20	36

Manchon acoustique 48 dB(A)

- manchon en Z,
- corps en tôle galvanisée constitué d'une partie fixe et d'une partie coulissante,
- traitement acoustique : laine de verre,
- auvent en matière plastique beige

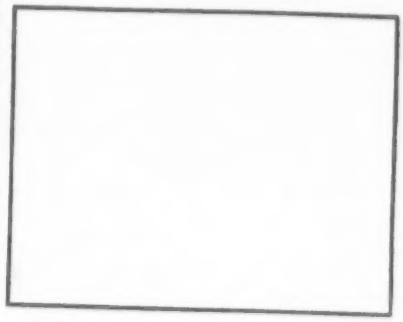

REMARQUES :

- Lors du scellement de la partie fixe du manchon, veiller à ne pas détériorer la laine de verre : empêcher toute pénétration de ciment ou laitance vers la laine de verre.
- Il est prudent d'assurer l'étanchéité entre l'auvent extérieur et la paroi par un mastic qui sera compressé lors du vissage de l'auvent.

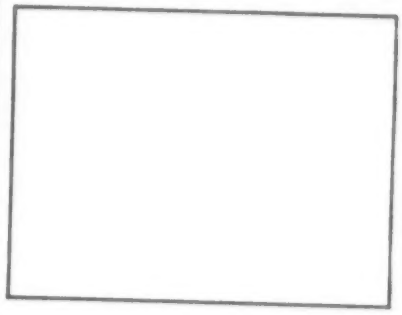

Isolement acoustique obtenu Dn (route) 48 dB(A).

Analyse par bande de fréquence : voir graphique.

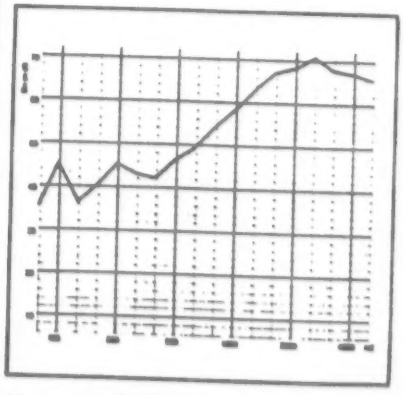

CODE	TYPE	A cm	B mini cm	B maxi cm
14011	Manchon acoustique Z HYGRO	16	23	35,5
14012	Manchon acoustique Z HYGRO	18	21,5	28

HAUT DE FENETRE

Manchon non acoustique
- corps en tôle galvanisée,
- flasque en aluminium anodisé,

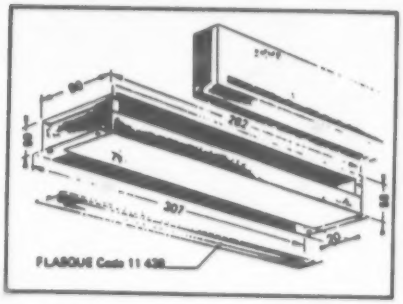

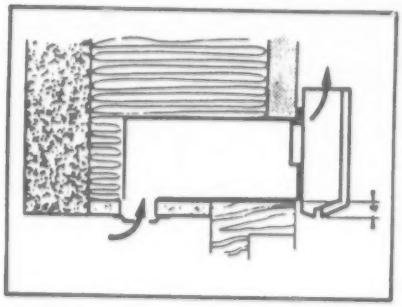

CODE	TYPE
14005	Manchon haut de fenêtre HYGRO

Manchon acoustique 38 dB(A)
- corps en tôle galvanisée,
- flasque en aluminium anodisé,
- traitement acoustique laine de verre.

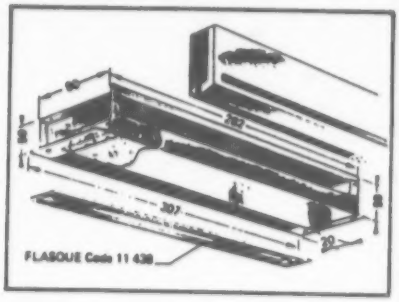

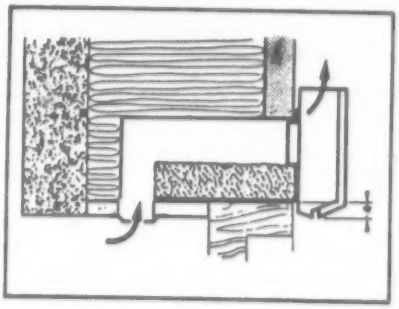

Isolement acoustique obtenu Dn (route) 38 dB(A).

Analyse par bande de fréquence : voir graphique.

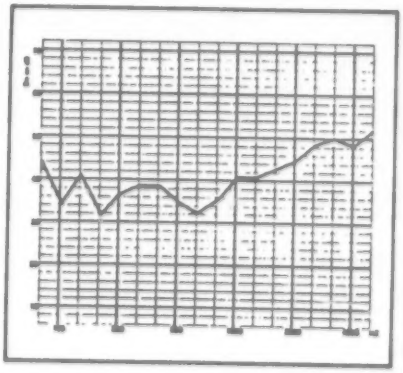

CODE	TYPE
14006	Manchon haut de fenêtre acoustique HYGRO

COMBLE

Cette mise en œuvre est réservée aux maisons individuelles possédant des combles ventilés.

Manchon comble
- corps en tôle galvanisée,
- filtre à très faible perte de charge,
- rallonge en tôle galvanisée.

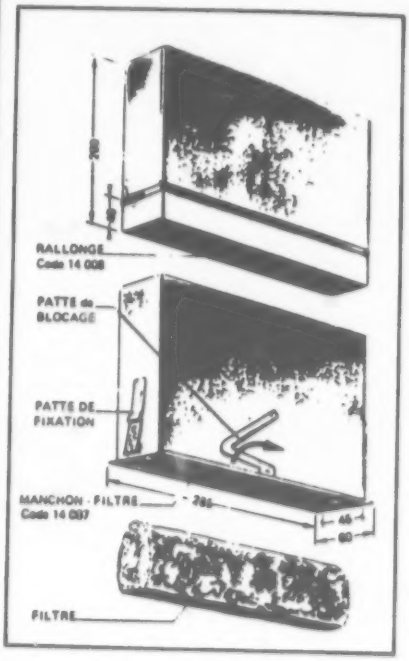

La rallonge perment en cas de laine de verre projetée d'éviter toute pénétration de laine de verre ou obstruction du manchon par celle-ci.

- Dans le placoplâtre
  1. visser les boutons à tête moletée,
  2. écarter les pattes de maintien latérales.
- Dans le cas d'une dalle on veillera à ne pas provoquer de déformation du manchon scellé afin de pouvoir glisser aisément une éventuelle rallonge.

NOTA : la mise en œuvre des entrées d'air en comble implique un raccordement obligatoire du refoulement à une sortie de toiture.

VMP K

MULTI-POINT MECHANICAL VENTILATION EXHAUST SYSTEM

DESCRIPTION

The VMP-K is a multi-point mechanical ventilating exhaust system. It was designed mainly for residential use. For this reason, this literature only pertains to this type of installation. The VMP-K may, however, be used as well in many other applications such as small professional buildings, service stations, etc.

In Residential Installations :

- Fresh air from the outside is brought into the bedrooms, dining room and living room through discreet self-regulating air inlets.
  N.B. : the use of self-regulating air inlets, in connection with the VMP-K, is not absolutely necessary except in the super-insulated home. The advantage of this type of inlet is that it assures the exact air change necessary, and thus allows the fan unit to operate in ideal conditions.
  In the case that the air inlets are not installed, cracking of windows and natural infiltration will in most cases assure the necessary fresh air intake.
- Polluted, stale inside air is exhausted from the bathrooms, powder rooms and kitchen by the VMP-K through air grilles and a ducting system. Most interior humidity problems are thus solved.

OBJECTIVES :

COMFORT, EFFICIENCY, ENERGY SAVINGS

The VMP-K is a quality product and the result of many years of research by ALDES to find the best answer to the ventilation problems in today's home. The highly efficient fan unit assures a healthy air change with the guarantee that the airflow rates in normal conditions will not be lower than those indicated for the unit.

And, this added comfort is obtained in an economical manner. Indeed, when compared with conventional fans or opened windows, the VMP-K saves energy.

The major advantages of the VMP-K are :

- A constant volume of air exhausted from the bathrooms and powder rooms.
- 2 extraction rates for the kitchen : a minimum of 35 cfm or 40 cfm, and 120 cfm.
- A very low noise level.
- Quickly and easily installed.
- Does away with ventilating fans in each bathroom or powder room.
- Complements the kitchen range hood.

The typical VMP-K installation for residences consists of :

- A fan unit.
- One exhaust outlet grille and sleeve for the kitchen.
- Exhaust outlet grilles and the corresponding sleeves for the bathrooms and powder rooms.
- The necessary ducting.
- Noise absorbing ducting for placing between fan unit and kitchen if necessary.
- Sound attenuators for placing on the bathroom and powder room duct runs if necessary.
- 0.2 hours timer.
- A cowl for exhausting air to the outside.

DESCRIPTION

FAN UNIT

1 VMPK-3

Housing

Made of polypropylene with :

One 6" diameter duct connector for kitchen.
Three to five 3" diameter duct connectors for bathrooms and powder rooms.
One 6" diameter exhaust-to-outside duct connector.

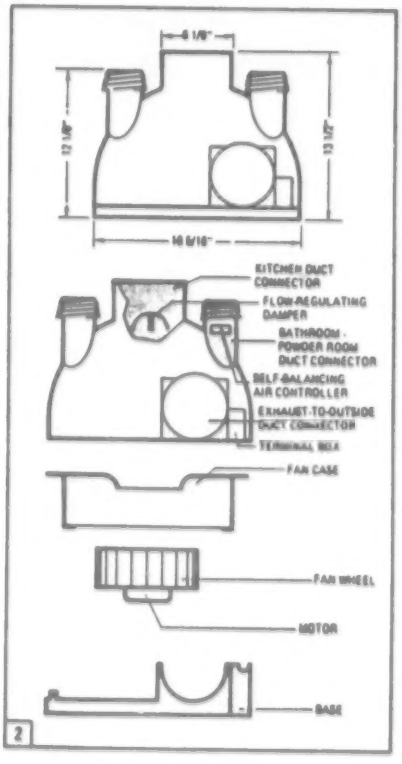

2

Three brackets for suspending or wall mounting the fan unit.
Weight : 12 lbs (5,5 kg) motor included.

Motor/Fan

Reversible centrifugal type which gives two different extraction rates depending on direction in which fan wheel rotates.

Single phase, 115 volts, 60 Hz.
One speed : 1800 rpm
Fan performance is stable between 103 and 127 volts for the 115 volts model.

Amps :
115 model : 0.6/1.0

Capacitors
115 model 8µF 250 rated/voltage

Maximum temperature rise : 140° F at 190 cfm.
Thermal overload protection (248° F)
Bearings lubricated and sealed for life
Horizontal or vertical positioning of motor possible.

Fan performance

See graph below.

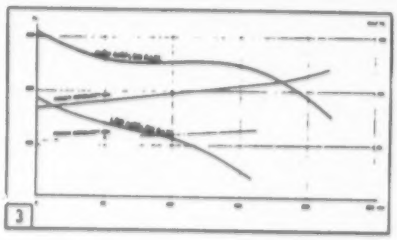

3

Wiring diagram

The electrical terminal box is located on the side. Access may be had by unscrewing hinged cover.

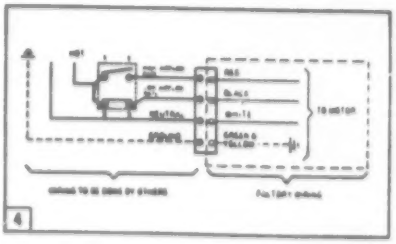

4

Sample installation in attic or basement

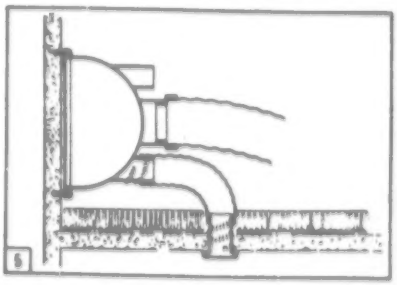

5

Kitchen exhaust

The fan unit provides 2 airflow rates for the kitchen by reversing the motor's direction of rotation. This results in :

- A low pressure airflow in one direction which gives a low extraction rate with reduced power consumption for normal conditions.
- A high pressure airflow in the other direction which gives a high extraction rate for use during meal-preparing-time.

The resulting airflow rate combined with an efficient flow-regulating damper give the following exhaust rates for the kitchen :

- Low exhaust rate : 35 cfm or 40 cfm depending on the model.
- High exhaust rate : 120 cfm. (Results are obtained with a clean filter).

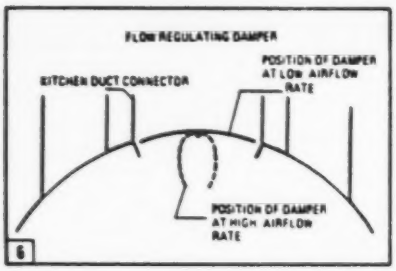
FLOW REGULATING DAMPER
KITCHEN DUCT CONNECTOR
POSITION OF DAMPER AT LOW AIRFLOW RATE
POSITION OF DAMPER AT HIGH AIRFLOW RATE
6

Duct connector for bathrooms and powder rooms

These 3" diameter duct connectors have self-balancing air controllers (ALDES patent) in their interior.

Whenever there is a pressure difference between the two sides of the air controller, the membrane, which is incorporated in this device, automatically adjusts the air passage, maintaining a constant airflow rate.

The result is :

- A constant airflow rate in the bathrooms and powder rooms despite changes in the kitchen exhaust rate.
- The automatic compensation of pressure drops in the ducting system. Consequently, no airflow adjustments are ever necessary.

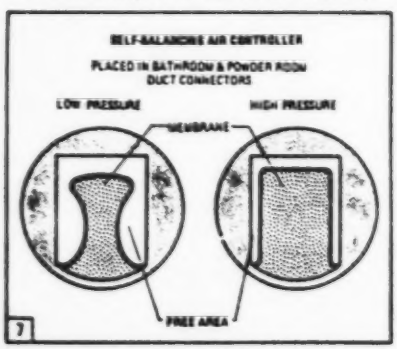

7

Two types of self-balancing air controllers may be used in the duct connectors :

- 10 cfm, 20 cfm.

The duct connectors (22 049) have threads for easily screwing on flexible plastic ducting.

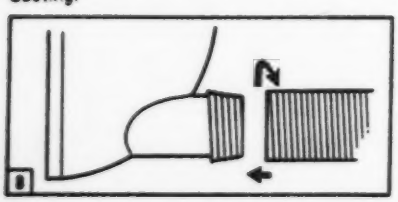
8

KITCHEN EXHAUST GRILLE 22 015
6" KITCHEN SLEEVE 22 013

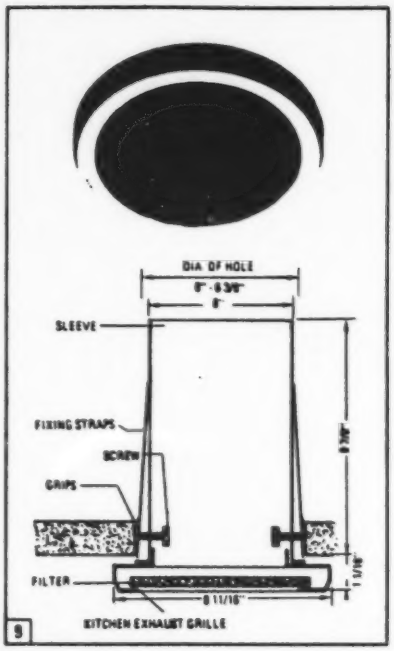

9

The kitchen exhaust grille is made of plastic and comes with a washable 1/2" filter which may be cleaned with an ordinary household detergent.

A specially designed 6" diameter sleeve is furnished in the kit. It is made of galvanized sheet metal.

The sleeve has a fastening system which assures an easy installation.

Diameter of hole : 6" to 6 3/8".

The grille is installed by simply snapping it into the sleeve.

The extraction rate for the kitchen exhaust grille is controlled by the flow-regulating damper placed inside the kitchen duct connector on the fan unit.

NOISE ABSORBING DUCT 22 012 (option)

This ducting is to be placed between the kitchen duct connector on the fan unit and the kitchen exhaust grille.

Length : 3 feet.

The ends are made to be easily snapped in

- On one end, to the 6 1/8" kitchen duct connector on the fan unit.
- On the other end, to the kitchen exhaust grille sleeve.

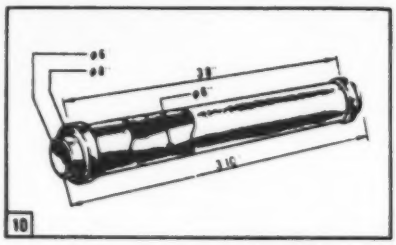
10

In this way, if the fan unit is placed directly over the kitchen, the noise absorbing duct may be used for hooking up the fan unit and kitchen exhaust grille.

When the distance between the fan unit and kitchen air grille is greater than 3'8", ordinary 6" flexible plastic ducting should be used to complete the ducting run.

The noise absorbing ducting creates no more pressure drop than the ordinary 6" flexible ducting.

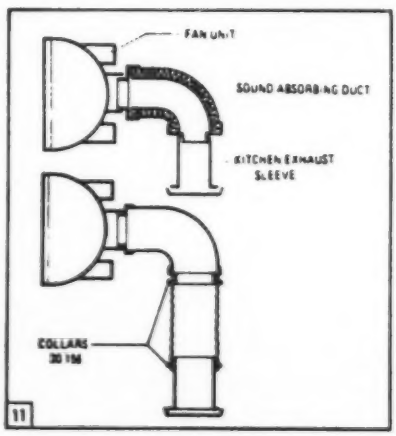

11

Noise absorbing characteristics

FREQUENCY (Hz)	63	125	250	500	1 000	2 000	4 000	8 000	Global
Sound absorbing duct (ϕ6")	dB	dB	dB	dB	dB	dB	dB	dB	dB(A)
Ordinary flexible ducting	67	71	80	74	82	77	71	58	84
Flexible duct + 1 length of sound absorbing duct	59	50	53	46	50	39	40	36	52
Sound attenuation	8	21	27	28	32	38	31	22	32

BATHROOM AND POWDER ROOM AIR OUTLETS

The outlet grille is made of plastic and is made to be inserted into a specially designed polypropylene sleeve (3" diameter) which has 3 interlocking extension elements. This sleeve may thus be shortened, or even lengthened, depending on ceiling or partition thickness. The sleeve is held in place by a blocking ring.

The sleeve is designed for 3" flexible plastic ducting, which is held on by the grippers on the sleeve. This ensures a snug fit.

Diameter of hole : 3 1/4" to 3 3/8".

The airflow rate for each bathroom and powder room is regulated by the self-balancing air controllers placed in the duct connectors on the fan unit.

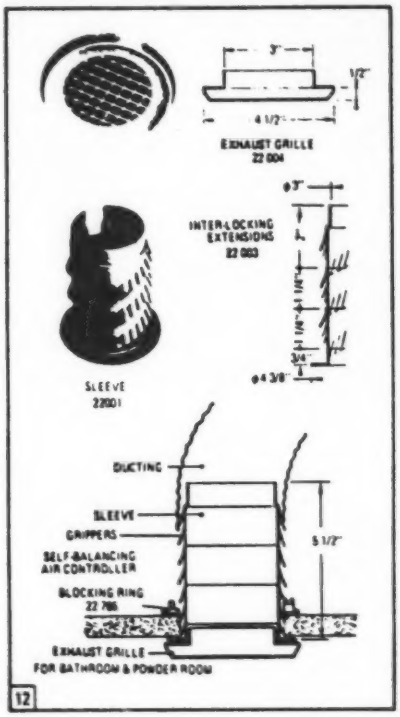

12

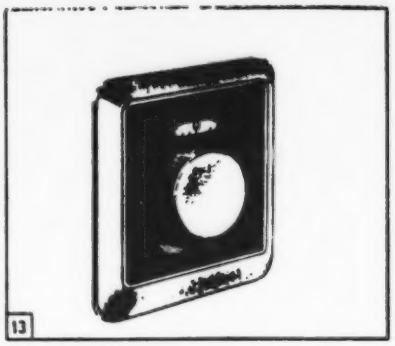
13

0.2 HOURS TIMER 29 018 (option)

The 0.2 Hours timer allows to increase the exhaust from the kitchen during 2 hours. This is obtained by reversing the rotation of the VMP-K fan.

SOUND ATTENUATOR (option)

They are for 3" duct and should be placed on the bathroom and powder room duct runs.

The sound attenuator is made of synthetic rubber.

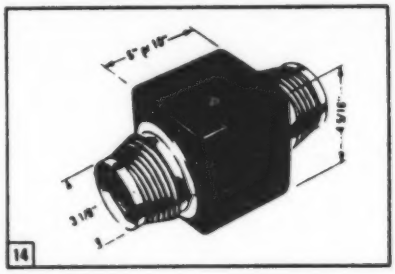
14

Each end of the sound attenuator has threads for screwing on the corresponding ducting.

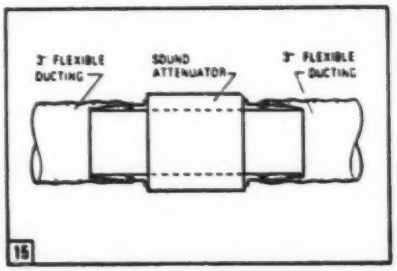

15

Sound attenuator 5" length 22 009
Sound attenuator 10" length 23 029

Noise absorbing characteristics

FREQUENCY (Hz)	63	125	250	500	1 000	2 000	4 000	8 000	Global
Sound attenuator (5" model)	dB	dB	dB	dB	dB	dB	dB	dB	db(A)
Flexible ducting	68	82	83	82	88	85	80	65	91
Flexible ducting w/attenuator	52	62	68	68	79	75	62	53	81
Sound attenuation	16	20	15	14	9	10	18	12	10

HIGH-LOW SPEED SWITCH

Electrical switches and boxes are not provided in the kit. A two speed switch may be installed in a convenient spot in the kitchen. It is to be wired in compliance with the local electrical code.

ACCESSORIES

To complete a VMP-K installation, ALDES can furnish the following :

- Flexible plastic ducting :
  - 3" for bathrooms and powder rooms.
  - 6" for kitchen and main exhaust to outside
- Roof cowls
- 0.2 hours timer.
- Rigid plastic flat ducting.

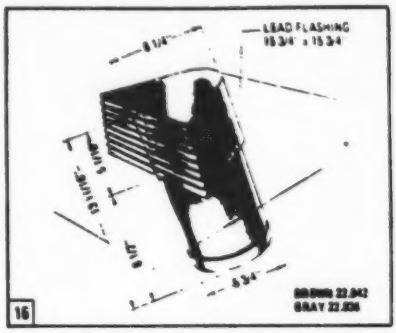

16

- Specially designed flat plastic ducting (1 5/8" x 4") : this type of ducting may be used where there is not enough space for passing ordinary 3" round ducting. The necessary connectors and ells are available

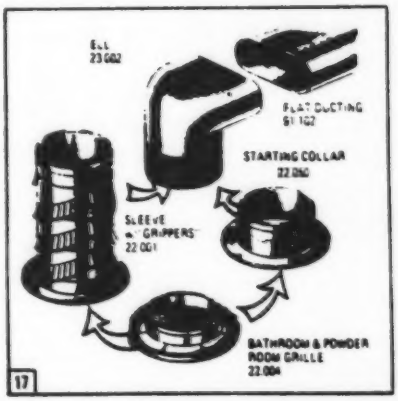

17

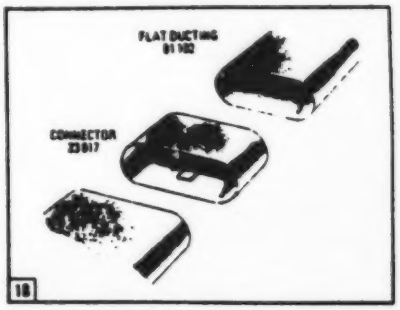

18

SOUND DATA

FAN UNIT

The noise level is measured in terms of sound pressure level, i.e., the sound that will be heard by a person placed at a certain distance from the fan unit. The indicated results are an average of 7 readings taken all around the fan unit.

Conditions of test :

- All duct connectors are hooked up to ducting.
- The air outlets and the main air exhaust outlet to the exterior are not situated in the room where the readings are made.
- The fan unit is placed on a rubber mat in the center of the testing facility.
- The microphone is placed 5' from the fan unit which is running at low speed.

FREQUENCY (Hz)	125	250	500	1 000	2 000	TOTAL dB(A)
SPL (dB)	48	46	44	38	33	44.5

AIR OUTLETS

The noise level for the air outlets is also given in terms of sound pressure level.

Conditions of test :

- Volume of room : 1 400 cu. ft.
- Reverberation time : 0.5 second.
- The kitchen grille is connected to the fan unit with a standard 3" sound absorbing length of ducting.
- Each bathroom and powder room outlet is installed with 10'9" of 3" diameter ordinary plastic flexible ducting with 1 sound attenuator for each length.
- The microphone is placed 5' from the air outlet.

		dB(A)	ISO	NC
LOW EXHAUST RATE	Kitchen 40 cfm	30	N 25	20
	1/2 bath 10 cfm	27	N 20	20
	Bathroom 20 cfm	28	N 20	20
HIGH EXHAUST RATE	Kitchen 120 cfm	38	N 35	35
	1/2 bath 10 cfm	31	N 20	20
	Bathroom 20 cfm	35	N 30	25

The results given above were obtained with a VMP-K3.

N.B. : the noise level of the air outlets is directly related to the length of the ducting. Thus, the longer the flexible plastic ducting, the quieter the system.

The following corrections may be made according to length :

- Kitchen : 1 dB(A) for each additional 3 ft. length of 6" flexible plastic ducting.
- Bathrooms and powder rooms : 0.5 dB(A) for each additional 3 ft. length of 3" flexible plastic ducting.

CONTENTS OF STANDARD KIT

Each kit includes the following components :

P/N		DESCRIPTION	VMP-K3	VMP-K5
VMP-K3	VMP-K5			
22 125	22 180	VMP-K kit		
22 875	22 653	Fan unit 115 V - 60 Hz	1	1
22 013	22 013	6" dia. kitchen exhaust sleeve	1	1
22 015	22 015	Kitchen exhaust grille	1	1
22 001	22 001	3" dia. sleeve w/«grippers»	3	5
22 004	22 004	3" dia. bathroom/powder room grille	3	5

(50 Hz models are available on special order)

AIRFLOWS cfm	LOW AIRFLOW RATE		HIGH AIRFLOW RATE	
	K3	K5	K3	K5
Kitchen	40	35	120	120
1/2 bath 10 cfm	2 x 10	3 x 10	2 x 10	3 x 10
Bathroom 20 cfm	1 x 20	2 x 20	1 x 20	2 x 20
TOTAL	**80**	**105**	**160**	**190**

AIRFLOW RATES

The above airflow rates are obtained under the following conditions :

- 22 ft. of ducting between the air outlet and the fan unit.
- 8 ft. of ducting for the stale air ducting between fan unit and the outside, and the use of a roofcowl at the end of this ducting.

OTHER INSTALLATION POSSIBILITIES AND APPLICATIONS

The typical installation given above may be varied in any number of way to fit individual needs.

For example, a combination bathroom-powder room-attic ventilation installation is possible. In this case, the 6 1/8" duct connector is used to extract the attic air.

Other applications include almost all situations where constant, efficient and silent ventilation is needed.

INSTALLATION

See our Installation - Operation - Maintenance literature.

It is very important to follow these instructions in order to assure that the VMP-K performs correctly and gives maximum satisfaction.

WARRANTY

The entire unit is guaranteed for 2 years, from date of shipment, against all manufacturing defects provided the material has been installed and operated under normal conditions. This warranty is limited to the repair or replacement of the material upon its return freight paid to our factory.

We reserve the right to change specifications without notice.

AMERICAN
ALDES
VENTILATION CORPORATION
Northgate Center Industrial Park
4539 Northgate Court
Sarasota, Florida 33580-4864
Phone (813) 351-3441
Telex 756533